# Topics in Stochastic Particle Systems and Self-Organised Criticality

Nanxin Wei

Supervised by Dr. Gunnar Pruessner

Department of Mathematics

Centre for Complex Science

Imperial College London

London SW7 2AZ

United Kingdom

A thesis is submitted for the degree of

Doctor of Philosophy of Imperial College London

February 2020

I certify that this thesis, and the research to which it refers, are the product of my own work, and that any ideas or quotations from the work of other people, published or otherwise, are fully acknowledged in accordance with the standard referencing practices of the discipline.

Signed: _____

# Copyright

The copyright of this thesis rests with the author and is made available under a Creative Commons Attribution Non-Commercial No Derivatives licence. Researchers are free to copy, distribute or transmit the thesis on the condition that they attribute it, that they do not use it for commercial purposes and that they do not alter, transform or build upon it. For any reuse or redistribution, researchers must make clear to others the licence terms of this work.

# Topics in Stochastic Particle Systems and Self-Organised Criticality


## Abstract

The thesis studies non-equilibrium stochastic particle systems, especially in the context of self-organised criticality. With increasing degree of complexity, different theoretical methods are explored, drawing upon the probability theory of branching processes and statistical field theory. The concept of "criticality" and its typical signatures are carefully examined in non-equilibrium complex systems and exactly calculated for branching particle systems to identify universal features beyond the universality class. New theoretical results on the critical density of Abelian Manna Model are found. Field theoretical approach is discussed to highlight the importance of dynamical correlations in certain models, and is generalised to accommodate critical reaction-diffusion processes on graphs.

*To my family.*

# Acknowledgments

The only immeasurable function that I encountered throughout the course of my PhD is my emotional debt to so many. Most significantly of course is to my supervisor Gunnar, who has supported me unswervingly despite everything, and without whom I truly cannot imagine going through the finishing line. In a shameful rush, here I only list some of the names that I owe my thanks to, from both academia and life:

Henrik, Tim, Bo, Saoirse, Ignacio, Johannes, Rosalba, Benjamin, Luca, Qing, Bingsheng, Letian, Simone, Max, Fabian, James, Ginestra, Ton, Peter, Reimer, Nicholas, Alvaro, Miguel, Mauricio, Renaud, Julien, Tibor, Chiu-Fan, Anderson, Lene, Sensen, Shale, Dong, Xinyuan, Mingzhen, ...

And last but equally global maximums of my emotional landscape, to Luo and my parents.

# List of Figures


3.1 The six different *active motives* of the one-dimensional Abelian Manna Model. The central site carries either three ($\alpha_i$ for $i = 0, 1, 2$) or two particles ($\beta_i$ for $i = 0, 1, 2$) and is to topple in the next microscopic time step. The occupation number of sites neighbouring the central site are representative only in as far as their parity is concerned, with $i$ indicating the number of sites that carry an odd number. Their occupation number is *post-toppling* (after *they* may have toppled themselves, but prior to the central site toppling), whereas the central site is shown *pre-topping* (before it topples). The configurations differ in whether neighbouring sites may or may not topple themselves due to being charged by the toppling site. Although we may picture the configurations being situated on a one-dimensional lattice, their spatial orientation is irrelevant and so we do not distinguish left and right neighbours. . . . . 43

3.2 Example of a toppling on a one-dimensional lattice. The initial state $\alpha_1$ goes over into state $\beta_2$ with probability (w.p.) $\zeta/4$, which is the joint probability of three independent events: The independent toppling of two particles to one side (w.p. 1/4) and the occupation of a next-nearest neighbouring site (w.p. $\zeta$). The latter assumption ignores spatial correlations. . . . . 44

3.3 Estimate of the asymptotic density in the fixed-energy version of AMM on random 5-regular graphs of different sizes. The approximate critical point, identified as the onset of asymptotic survival, at around $\zeta_c = 0.62$ is very close to the theoretical prediction $\zeta_c = \frac{1}{2} + \frac{1}{2q} = 0.6$. . . . . 49

5.1 Examples of $\mu$ vs. $\nu$, ER networks with $z = 5$, fixed fractional threshold $\hat{\theta} \equiv \theta$ . . . . . 71

5.2 Phase diagram of WTM on ER networks . . . . . 72

5.3 WTM on fixed finite network . . . . . 76

5.4 Illustration of two phases of networks under the persistent dynamics . . . . . 79
5.5 Schematic illustration of the effective dynamics in contrast to the model dynamics . . . . . 81
5.6 $\rho(R)$ from effective trigger size of steady state . . . . . 82
5.7 $R$ vs. $\rho^*$ in the stationary phase, theoretical estimates and simulation results . . . . . 84
5.8 $R$ vs. $t_c$ in the collapsing phase, theoretical estimates and simulation results . . . . . 85

# List of Tables

3.1 Branching probabilities of active motives on a regular lattice with constant coordination number $q$. The only form of branching occurs is when two independent copies of $\beta_k$ are generated, indicated by $2\beta_k$. The symbol $\varnothing$ indicates that no offspring is produced. . . . . 45

3.2 The theoretical estimate of the critical density $\zeta_c$ in the $d$-dimensional AMM derived here compared to the numerical values reported in the literature for the stationary density of the Abelian Manna Model. . . . . 48

# Contents


**0** Introduction **1**

**1** Absorbing Phase Transition, Critical Avalanches and Branching Processes **5**

1.1 APT and Critical Avalanches . . . . . 5

1.2 Universality of Branching Processes . . . . . 8

1.2.1 Homogeneous Markov BP . . . . . 9

1.2.2 Inhomogeneous Markov BP . . . . . 17

1.2.3 Age-dependent BP . . . . . 18

1.2.4 BP with immigration . . . . . 25

1.3 Summary Remarks . . . . . 27

**2** Absorbing Phase Transitions and Finite-Time Properties of Spatial Branching Processes **29**

2.1 Some Results and Remarks on APT of Spatial BP . . . . . 30

2.1.1 Branching diffusions in bounded domains . . . . . 30

2.1.2 Branching diffusions with drift on the half line . . . . . 31

2.2 Finite-Time Properties of Spatial BP . . . . . 33

**3** Multi-Type Branching Process as Effective Mean-Field Theory of Abelian Manna Model **38**

3.1 Abelian Manna Model and Self-Organised Branching Process . 39

3.2 Self-Organised Multi-Type Branching Process and the Critical Density of AMM . . . . . 42

3.2.1 The fixed-energy AMM on random regular graphs . . . 48

3.3 Summary and Discussion . . . . . 50

**4 Field-Theoretic Approach to Reacting Particle Systems 52**

4.1 Brief Introduction to the Doi-Peliti Formalism of Field Theories 53

4.2 Examples of Field Theories *à la* Doi-Peliti . . . . . 57

4.2.1 Field theory of activated random walk . . . . . 57

4.2.2 Field theory of branching Wiener sausages . . . . . 58

4.3 Critical Dynamics of Reacting Diffusive Particle Systems on Networks . . . . . 60

**5 Threshold Dynamics on Complex Networks and Message-Passing Methods 65**

5.1 Watts Threshold Model and Abrupt Transitions . . . . . 66

5.1.1 WTM on random networks . . . . . 67

5.1.2 WTM on fixed finite network . . . . . 73

5.2 Persistent Threshold Dynamics with Recovery on Random Networks . . . . . 77

5.2.1 Model set-up and general behaviour . . . . . 78

5.2.2 Effective trigger size evolution of the persistent dynamics 79

5.2.3 Results and discussions . . . . . 83

**6 Summary 87**

**Bibliography 103**

# 0 Introduction

The thesis is dedicated to the analysis of a few probabilistic models loosely under the umbrella of *stochastic particle systems* (SPS) [1, 2] and the development of theoretical methods for more general purposes. SPS are a wide class of mathematical models originated from the studies of complex systems [3, 4], which from a statistical physics point of view, are systems consisting of many components interacting with each other and/or the environment under simple dynamical rules, with relevant macroscopic phenomena explained as emerging from the collective behaviour of their components. In models, components are sometimes treated as "particles", no matter whether they are particles in the physical sense [5] or abstraction that retains the discreteness and other key properties of the components, e.g., individuals in population dynamics or epidemic models [6]. Dynamical rules of the particles are often chosen to be "stochastic", either of intrinsic quantum mechanical origin [7] or due to the fact that details of the interaction involving components (particles) are too complicated to track, while statistical observables are sufficient to account for the macroscopic phenomena of interest. Such models that feature particles as discrete entities and stochastic dynamics are what we referred to as SPS. Many of these models are often studied under the name

of *interacting particle systems* [8, 9]. We prefer SPS to include models such as branching particle systems and random walkers [2] where particles don't interact with each other explicitly. Also throughout the thesis, we refer to stochastic dynamical rules of particles as *microscopic* dynamics and consider as the starting point of our inquiry, even if such dynamical rules may be extracted from *coarse-graining* upon mechanisms in smaller scales and are in some sense *mesoscopic* [1].

SPS can be roughly categorised into *(i)* reaction particle systems and *(ii)* spin particle systems. The former often arises from the backgrounds of chemical reactions, population dynamics, epidemics, etc. [5, 2], where particles are endowed with intrinsic properties called *species* or *types*. Particle number doesn't necessarily conserve in reactions. When spatial degrees of freedom are concerned, particles may move around or hopping among different sites. The latter are associated with applications where particles are bound to their spatial or topological positions, such as in (kinetic) Ising model, voter model [2] or neural networks [10]. Particles adopt different *states* following the microscopic dynamics, while the total particle number is conserved. Note that such division is not absolute, a system may be modelled in either way depending on the perspective. For example, we can construct both metapopulation model (reaction-like) and individual-based model (spin-like) for epidemics [6, 11]. Also, a spin particle system, when only certain spin states are of interest, may be treated as effectively a reaction particle system with mobile particles representing the spatial evolution of spin states. In the current thesis, we focus on methods for reaction particle systems, which by extension are relevant for models that can be mapped into reaction particle systems as well.

Reaction particle systems are often *non-equilibrium*, as the transitions between macroscopic states (configurations) of the system may break *detailed balance* [12, 2]. This is apparent for systems with *absorbing states*, where the system stops evolving once entering such a state. Whether a system would end up in one of its absorbing states is typically contingent on some macro-

scopic observable (control parameter), leading to the study of *absorbing phase transition* (APT), and further dynamical critical behaviours around the transition [13, 14, 12, 15]. APT is not only important for many applications of complex system modelling, e.g., extinction or fixation of populations [16], outbreak of epidemics [6], information cascades [17, 18], neural avalanches [19], etc., but also poses interesting theoretical questions due to the significance of fluctuation near criticality and the how discreteness of particles features in such transition. In particular, we are interested in models with microscopic dynamics coupled to some macroscopic feedback mechanism that *self-organise* the system into its criticality without the need of *fine-tuning* the control parameter. These are models known to present *self-organised criticality* (SOC) [20, 21]. Paradigmatic models of SOC are cellular automata with simple dynamical rules of separate time-scales and prescribed boundary conditions, which demonstrate rich phenomenology (critical behaviours sensitive to subtle changes in the dynamical rules, some of which remain controversial) while largely lacking exact solutions [22].

Despite the simplicity of microscopic dynamics, SPS are usually challenging to solve directly. Apart from a few special cases, the standard analytical treatment of SPS resorts to (further) coarse-graining to smooth out particle discreteness and stochasticity [12, 15]. In the first step, all fluctuations are ignored, resulting in a deterministic *mean-field theory* (MFT) of the system. Then appropriate noise is introduced to capture the (main) effects of stochasticity of the microscopic dynamics and the critical behaviours of the model. In this thesis we explore methods for SPS from a different approach, trying to hold on to particle discreteness and stochasticity as much as possible, while relaxing, at different levels, spatial-temporal correlations to keep the models analytical tractable. When all the dynamical correlations (spatial-temporal correlations due to particle interactions) are ignored, particles with only self-reactions form *branching processes* (BP) [2, 23]. In **Chapter 1** and **Chapter 2**, we discuss a few classes of BP and spatial BP as candidates for non-trivial MFT, challenging some of the commonly held presumptions of MFT in non-equilibrium systems [12, 24]. We then move to showcase in **Chapter 3** incorporating short-range dynamical correlations of an SOC

model in an effective BP which is exactly solvable, giving closed-form approximates of a key quantity of the model in generic set-ups. We introduce and develop field-theoretic methods to tackle long-range dynamical correlations in **Chapter 4**, and conclude in **Chapter 5** with the application of a systematic way to ignore correlations for network dynamics and some fresh results.

# 1

# Absorbing Phase Transition, Critical Avalanches and Branching Processes

This chapter is partially based on the article [25] "*Comment on 'Finite-size scaling of survival probability in branching processes'* ", Physical Review E 94.6 (2016): 066101, by Nanxin Wei and Gunnar Pruessner.
NW is the main contributor to the article.

## 1.1 APT and Critical Avalanches

We consider systems with absorbing-state(s) and one species of *active* particles and refer to the population of active particles at time $t$ and the population size $N(t)$ both as *activity* as long as the indication from context is clear. Without activity, the system is in an absorbing state, i.e., stops evolving. If initiated with $N(0) > 0$ (typically $N(0) = 1$), the (eventual) survival probability of activity $P_a^* := \lim_{t\to\infty} \mathbb{P}\{N(t) > 0\}$ satisfies

$$P_a^* \qquad \begin{cases} = 0 & m \leqslant m_c \\ > 0 & m > m_c \end{cases} \tag{1.1.1}$$

where $m$ is some effective control parameter characterising the SPS, we say the system admits an *absorbing phase transition* (APT), with $m \leqslant m_c$ in the *absorbing phase* and $m > m_c$ in the *active phase*. If further in the active phase

$$P_a^*(m) \sim |m - m_c|^{\beta'} \tag{1.1.2}$$

then the APT is continuous and $m_c$ the critical point of the phase transition. At the critical point of a continuous APT, observables are expected to be scale-invariant and display algebraic relation in their asymptotes, most prominently featured in the finite-time active (survival) probability $P_a(t) := \mathbb{P}\{N(t) > 0\}$ and the mean activity $\mu(t) := \langle N(t) \rangle$,

$$P_a(t) \sim t^{-\delta} \tag{1.1.3}$$

$$\mu(t) \sim t^{\theta} \tag{1.1.4}$$

According to theory of critical phenomena, without spatial degree of freedom, the three exponents $\beta$, $\delta$, $\theta$ determine the universality class of the APT (among which $\delta$ and $\theta$ are dynamic exponents at criticality) [13, 12].

When the system from an absorbing (or quiescent) state is *driven* to take up some initial activity, the evolution of activity until its termination (the system entering an absorbing state again) can be perceived as an *avalanche*. Of particular interest are critical avalanches with the underlying activity process poised at or near the critical point of the APT. Critical avalanches are expected to exhibit scale-invariant distributions of avalanches size and duration:

$$P_{\mathcal{T}}(T) \sim T^{-\tau_{\mathrm{T}}} \mathcal{G}_{\mathrm{T}}(T/T_c) \tag{1.1.5}$$

$$P_{\mathcal{S}}(S) \sim S^{-\tau_{\mathrm{S}}} \mathcal{G}_{\mathrm{S}}(S/S_c) \tag{1.1.6}$$

where $\mathcal{S} := \int_0^\infty N(t)dt$ and $\mathcal{T} := \inf\{T : N(T) = 0\}$ are avalanche size and duration respectively; $S_c$ and $T_c$ are characteristic avalanches size and duration (cut-off of power-law) dependent on the system size and distance to the critical point, diverging at thermodynamic limit when approaching criticality. A more refined ansatz on critical avalanches link the statistics of size and duration:

$$\langle \mathcal{S}|dT\rangle := \mathbb{E}\{\mathcal{S}|\mathcal{T} \in (T-dT, T]\} \sim T^{\gamma_{ST}} \tag{1.1.7}$$

which infers the conditional distribution

$$P_{\mathcal{S}}(S|dT) \sim T^{-\gamma_{ST}}\mathcal{G}_{ST}(S/T^{\gamma_{ST}}) \tag{1.1.8}$$

The activity process at criticality features only two independent dynamic exponents $\delta$ and $\theta$, which can be linked to the exponents of critical avalanches through scaling laws:

$$\tau_T = 1 + \delta \tag{1.1.9}$$

$$\tau_S = 1 + \frac{\delta}{1+\theta+\delta} \tag{1.1.10}$$

$$\gamma_{ST} = \frac{\tau_T - 1}{\tau_S - 1} = 1 + \theta + \delta \tag{1.1.11}$$

When avalanches are used as models for complex systems, the scaling relations in Eq.(1.1.5)–(1.1.7) are often considered as signatures of criticality. In addition, since the conditional expectation of avalanche size is the integral of the conditional expectation of activity $\mu(t|dT) := \langle N(t|dT)\rangle = \mathbb{E}\{N(t)|\mathcal{T} \in (T-dT, T]\}$, the latter, often regarded as (average) *temporal profile* of avalanches [26, 27], is also expected to take a scaling form at criticality

$$\mu(t|dT) \sim T^{\sigma}\Lambda(t/T) \tag{1.1.12}$$

with exponent $\sigma = \gamma_{ST} - 1 = \theta + \delta$ resulting from the scale-invariance of the two-time correlation function of the activity. The universal scaling function in rescaled time $\Lambda(t/T)$ is the so-called shape of the temporal profile or the *avalanche shape*, which has recently been purported as an additional

key indicator of criticality, especially when the power-law distribution of avalanche size or duration may emerge from non-critical dynamics [28, 29].

Systems with SOC feature statistics of critical avalanches, which can often be explained through some associated APT [30, 31]. Suppose there is a system with APT, where activity evolves at a fast or microscopic time-scale; If driving and dissipation at a slow or macroscopic time-scale establish a feedback mechanism making the critical point of the APT an attractor (stable fixed-point), the system would be *self-organised* to criticality from a range of initial conditions without *fine-tuning*. This mechanism occurs repeatedly in the later chapters of the thesis.

## 1.2 Universality of Branching Processes

Branching processes (BP) are reacting particle systems with only mono-particle reactions called *branching*. Throughout the thesis, we do not consider genealogical information and restrict our attention to the population dynamics of branching particle systems. From the mathematical perspective, BP bear the nice property of *additive independence* and are thus amenable to a number of analytical tools; From the modelling point of view, particles in BP have no explicit interactions and are often considered as mean-field theories (MFT) for more complicated interacting particle systems. As such, BP are extensively studied and have numerous applications from biology, physics to social sciences [32, 23, 33, 34, 35].

BP are also perhaps the simplest stochastic particle systems with continuous APT and natural candidates for modelling critical avalanches, widely believed to be subject to the universal mean-field critical behaviours in statistical physics literatures [12] and account for many observed power-law avalanche statistics with size exponent 3/2 [24].

In this section, we examine the APT and associated critical behaviours of a few typical classes of BP, with a special focus on observables conditioned on extinction or given extinction time, scenarios which link BP to avalanches. We provide an integral account to demonstrate the universality of mean-field critical behaviours of BP, both standard and non-standard, from the statistical physics perspective, while including the ingredients that are usually left out in the discussions of critical phenomena.

### 1.2.1 Homogeneous Markov BP

Consider single species (or one-dimensional) continuous-time BP $\{N(t)\}_{t\geqslant 0}$ initiated with one particle $N(0) = 1$. Homogeneous Markov BP is characterised by a branching rate $r$ and a random variable $K$ taking value from non-negative integers $\mathbb{N}$ representing the number of offspring produced per branching. At any time $t \geqslant 0$, each existing particle is independently subject to branching (Poissonian events) with rate $r$, when it is replaced by $K$ identical offspring. Let $\{p_k\}_{k=0,1,\dots}$ be the probability mass function of $K$ and $f(z) := \mathbb{E}[z^K]$, $z \in [0,1]$ its probability generating function, also referred to as *branching mechanism*. Throughout this chapter we only consider BP with finite mean offspring number and both positive death and birth probabilities by assuming that $m := \mathbb{E}(K) = f'(1) < \infty$ and $p_0 > 0$, $p_0 + p_1 < 1$.

Markovianity of $\{N(t)\}$ indicates that at any time $t$ all existing particles are equal in terms of branching, i.e., have the same branching rate and branching mechanism; Homogeneity further dictates that both the branching rate and branching mechanism are invariant over time. Define $P(n,t) := \mathbb{P}\{N(t) = n\}$, the BP satisfies master equation

$$\frac{\mathrm{d}P(n,t)}{\mathrm{d}t} = r\sum_k p_k(n-k+1)P(n-k+1,t) - rnP(n,t), \tag{1.2.1}$$

hence its generating function $F(z,t) := \mathbb{E}[z^{N(t)}]$, $z \in [0,1]$ satisfies the forward Kolmogorov equation

$$\begin{aligned} &\frac{\partial F}{\partial t} = r\frac{\partial F}{\partial z}[f(z) - z] \\ &F(z,0) = z, \end{aligned} \tag{1.2.2}$$

which can solved by the method of characteristics [36].

Homogeneous Markov BP are also naturally *renewal*, i.e., after the first branching event, the system is "renewed" to a collection of independent subsystems identical to the original one (with the same law).
Denote the life-time of a particle as $\tau$ and the life-time distribution $G(t) := \mathbb{P}\{\tau \leqslant t\} = 1 - e^{-rt}$, we have

$$P(n,t) = \delta_{n,1}[1 - G(t)] + \int_0^t dG(t_1) \sum_k p_k P^{*k}(n, t - t_1), \tag{1.2.3}$$

where $P^{*k}$ stands for the $k$-th convolution of $P(n,\cdot)$, followed by (the integral form of) the renewal equation:

$$\begin{aligned} &F(z,t) = z[1 - G(t)] + \int_0^t dG(t_1) f[F(z, t - t_1)] \\ &F(z,0) = z, \end{aligned} \tag{1.2.4}$$

which is equivalent to the backward Kolmogorov equation with the same initial condition

$$\begin{aligned} &\frac{\partial}{\partial t} F(z,t) = r[f(F(z,t)) - F(z,t)] \\ &F(z,0) = z. \end{aligned} \tag{1.2.5}$$

Let finite-time extinction probability be $Q(t) := F(0,t)$ and (eventual) extinction probability $q := Q(\infty)$. From Eq.(1.2.4) (even with general $G(t)$) we have

**Theorem 1.** (i) *$q$ is the smallest root of $f(z) = z$ in $[0,1]$, which exists.*

(ii) *If* $m = f'(1) > 1$, *then* $q < 1$; *Otherwise* $q = 1$.
*BP with* $m >< = 1$ *are referred to as super-, sub-, critical respectively.*

which can be further strengthened by

**Theorem 2.** (i) *If* $z \in [0, q]$, *then* $F(z,t) \uparrow q$, $t \to \infty$;
(ii) *If* $z \in (q, 1)$, *then* $F(z,t) \downarrow q$, $t \to \infty$.

Both Theorem 1 and Theorem 2 are standard results in the theory of BP, see for example [23].

Initial value problems Eq.(1.2.2) and Eq.(1.2.4) (with $G(t) = 1 - e^{-rt}$) both have the unique solution $F(z,t)$ and are equivalent in this case. Although the exact solution of $F(z,t)$ depends on details of the branching mechanism $f(z)$ and may not be easily obtained explicitly, its large $t$ asymptote adopts a unified closed form for all $z \in [0, 1)$ thanks to Theorem 1 and Theorem 2. In the rest of the subsection, we derive the large $t$ asymptote of $F(z,t)$ and the resulted observables of BP for two general classes of branching mechanisms.

#### 1.2.1.1 Regular branching mechanism

By "regular branching mechanism" we refer to offspring distributions with all moments finite, which indicates that $f(z)$ is analytic on $z \in [0, 1]$. This is also the most commonly used class of BP in applications, including the binary BP with $f(z)$ truncated at the second order.

- **(Eventual) survival probability**

$f(z)$ is Taylor expandable if it is analytic. For supercritical BP close to criticality, $q \uparrow 1$, we have

$$q = f(q) = 1 - m(1-q) + m_2(1-q)^2 + o\big((1-q)^2\big), \tag{1.2.6}$$

where $m_2 = f''(1)/2 < \infty$. Hence the survival probability and associated exponent $\beta'$ are given by

$$\begin{aligned} & P_a^* = 1 - q \simeq \frac{m-1}{m_2} \\ \Rightarrow \qquad & \beta' = 1 \end{aligned} \tag{1.2.7}$$

To obtain the large $t$ asymptotic solution of $F(z,t)$, it is convenient to work with the backward Kolmogorov equation Eq.(1.2.5). Since Theorem 2 ensures that when $t \to \infty$, $F(z,t) \uparrow q \ \forall z \in [0,q]$, define $\overline{F}(z,t) := q - F(z,t)$, then $\overline{F}(z,t) \downarrow 0$. Expand $f(\bullet)$ around $q$, for large $t$ and given $z \in [0,q]$, Eq.(1.2.7) can be approximated by

$$\begin{aligned} & \frac{dF}{dt} \simeq r[q - \tilde{m}(q-F) + \tilde{m}_2(q-F)^2 - F] \\ \Rightarrow \qquad & -\frac{d\overline{F}}{dt} \simeq r[\tilde{\epsilon}\overline{F} + m_2\overline{F}^2], \end{aligned} \tag{1.2.8}$$

where $\tilde{m} = f'(q)$, $\tilde{m}_2 = f''(q)/2$ and $\tilde{\epsilon} = q - \tilde{m} \geqslant 0$, which can then be solved by integration, with the initial condition $\overline{F}(z,0) = q - z$. The asymptotic solution reads

$$\overline{F}(z,t) \simeq \begin{cases} \frac{\tilde{\epsilon}(q-z)}{[\tilde{m}_2(q-z)+\tilde{\epsilon}]e^{\tilde{\epsilon}rt} - \tilde{m}_2(q-z)} & \text{sub- or super- critical} \\ \frac{1}{\tilde{m}_2 rt + 1/(q-z)} & \text{critical} \end{cases} \tag{1.2.9}$$

which contains the full information of the leading order contribution to the marginal distribution of the BP, $P(n,t)$, hence the asymptotes of all one-time observables. In the homogeneous Markov case, solution Eq.(1.2.9) conveniently encodes the large $t$ asymptotes of all multiple-time observables as well.

**• One-time observables**

For critical and subcritical BP, $q = 1$, Eq.(1.2.9) holds for $z \in [0,1]$, $\overline{F}(z,t)$ encodes the asymptotes of the probability distribution of $N(t)$ for large $t$,

from which we can extract all one-time observables. At criticality we have

$$\begin{aligned} & P_a(t) = \overline{F}(0,t) \sim 1/t \qquad (1.2.10) \\ \Rightarrow \quad & \delta = 1, \end{aligned}$$

and

$$\begin{aligned} & \mu(t) = -\overline{F}'(1,t) \equiv 1 \qquad (1.2.11) \\ \Rightarrow \quad & \theta = 0. \end{aligned}$$

Eq.(1.2.6),(1.2.10),(1.2.11) give the well-known mean-field exponents of APT.

For supercritical BP, $q < 1$, Eq.(1.2.9) holds on $z \in [0, q]$. The finite-time survival probability $P_a(t) = 1 - F(0,t) = 1 - q + \overline{F}(0,t)$, therefore follows exactly the same scaling form as subcritical BP but with a shift of the reference point $(1-q)$.

For supercritical BP to be avalanches, one should condition the processes on finite extinction time. Since $\mathbb{P}\{N(t) = n \,|\, \mathcal{T} < \infty\} = \mathbb{P}\{N(t) = n\}q^n$ due to the Markov property, we have

$$F(z, t|\mathcal{T} < \infty) = F(qz, t), \qquad (1.2.12)$$

therefore observables evaluated at $z = 1$ for the conditional process can be translated into evaluation at $z = q$ for the original process. E.g.,

$$\langle N(t|\mathcal{T} < \infty)\rangle = qF'(q,t) = qe^{-\tilde{\epsilon}rt} \qquad (1.2.13)$$

Conditional on extinction, the expected population size supercritical BP decays exponentially, just as subcritical BP.

- **Two-time observables**

  Thanks to the Markov property, the generating function of $n$-time joint

distribution of the BP can be directly written down in terms of $F(z,t)$, e.g.,

$$F_{12}(z_1,z_2,t_1,t_2) := \mathbb{E}[z_1^{N(t_1)} z_2^{N(t_2)}] = F(z_1 F(z_2, t_2 - t_1), t_1), \quad t_1 \leqslant t_2 \tag{1.2.14}$$

Asymptotes of the two-time observables can all be extracted from the asymptotic form of the (one-time) generating function $F(z,t)$ based on Eq.(1.2.9). In particular, we would like to characterise the temporal profile of avalanches $\mu(t|dT) := \langle N(t|dT)\rangle$ and the cumulated temporal profile $\mu(t|T) := \langle N(t|T)\rangle$, which are the expected number of particles at $t$ for BP conditioned on extinction at $T$ or by $T$ respectively. Since

$$\begin{aligned}\mathbb{P}\{N(t) = n \,|\, \mathcal{T} \in dT\} &= \frac{d\mathbb{P}\{N(t) = n,\, \mathcal{T} \leqslant T\}/dT}{dQ(T)/dT} \\ &= \frac{d[\mathbb{P}\{N(t) = n \,|\, \mathcal{T} \leqslant T\}Q(T)]/dT}{dQ(T)/dT},\end{aligned} \tag{1.2.15}$$

the temporal profile and its cumulated version are linked by

$$\mu(t|dT) = \frac{d[\mu(t|T)Q(T)]/dT}{Q'(T)} \tag{1.2.16}$$

The generating function for the BP conditional on extinction by $T$ is given by

$$F(z,t|T) := \mathbb{E}[z^{N(t|T)}] = \frac{1}{Q(T)} F(zQ(T-t), t), \tag{1.2.17}$$

hence

$$\mu(t|T) = F'(1,t|T) = \frac{Q(T-t)}{Q(T)} \frac{Q'(T)}{Q'(T-t)}. \tag{1.2.18}$$

Therefore from Eq.(1.2.16)

$$\mu(t|dT) = 1 + \frac{Q(T-t)}{Q'(T)} \frac{d}{dT}\left[\frac{Q'(T)}{Q'(T-t)}\right] \tag{1.2.19}$$

The first term on the right hand side of Eq.(1.2.19) is due to setting $N(0) = 1$ and $N(T) = 0$. To symmetrise with $\mu(t|dT^-) = \mu(t|dT) - 1$, or consider the shape of the temporal profiles which is rescaled to normalisation at large $T$, this term can be ignored. The second term is only dependent on the

finite-time extinction probability. At criticality, from Eq.(1.2.9) we have $Q(t) \simeq 1 - 1/(\tilde{m}_2 rt + 1)$, therefore

$$\mu(t|dT) \sim T\frac{t}{T}(1 - \frac{t}{T}), \tag{1.2.20}$$

with parabolic avalanche shape $\Lambda(x) = x(1-x)$ and consistent scaling exponent $\sigma = \delta + \theta = 1$.

• **Avalanche size**

Moments of avalanche size can be obtained by integrating moments of activity over time. The avalanche size distribution can also be derived directly from its generating function $F_S(z) := \mathbb{E}[z^{\mathcal{S}}]$, $z \in [0, 1]$ or moment generating function $\mathcal{M}_S(y) := \mathbb{E}[e^{-y\mathcal{S}}]$, $y = -\ln z \geqslant 0$ which satisfies

$$\mathcal{M}_S = \frac{1}{1+y} f(\mathcal{M}_S) \tag{1.2.21}$$

At criticality, in Eq.(1.2.21) expand $f(\bullet)$ around 1 to quadratic terms and solve the resulted equation, we have $P_{\mathcal{S}}(S) \sim S^{-3/2}$, hence $\tau_s = 3/2$, consistent with the scaling law Eq.(1.1.10).

All of the observables considered above, as far as their large $t$ (and $T$) asymptotes are concerned, only depend on the offspring number distribution up to its second (factorial) moments, leading to *universal* mean-field behaviours. These results can be understood from a more intuitive perspective: For homogeneous Markov BP, branching rate $r$ can be seen as a uniform rescaling of time, all the relevant information about the dynamics is encoded in the branching mechanism $f(z)$; If the branching mechanism is regular, $f(z)$ is analytic in $[0, 1]$ and plays a similar role to the analytic free energy in the Landau mean-field theory for continuous phase transitions in equilibrium systems, whose first derivative determines the critical point and the second derivative prescribes the mean-field critical behaviours.

#### 1.2.1.2 Branching mechanism with divergent variance

This corresponds to the offspring number $K$ having divergent variance, equivalently $\mathbb{E}(K^2) \to \infty$ (or $f''(1) \to \infty$), which often arises from avalanches on scale-free networks [27, 29]. Assume that $K$ adopts a power-law distribution, $p_k \sim k^{-\gamma}$ as $k \to \infty$ with $2 < \gamma < 3$. Eq.(1.2.4) still holds, so do Theorem 1 and 2. $m = 1$ is still the critical point of the BP, but $f(z)$ is no longer analytic at 1. Nonetheless, we can still asymptotically expand $f(z)$ around 1 [37]:

$$f(z) \simeq 1 - m(1-z) + c\Gamma(1-\gamma)(1-z)^{\gamma-1} \qquad z \to 1^- \tag{1.2.22}$$

where $\Gamma$ is the Gamma function and $c$ some constant. All the analysis for the regular Markov BP carries through by replacing the quadratic term with the power $(\gamma - 1)$ term, hence we have

$$P_a^* \sim |m-1|^{\frac{1}{\gamma-2}} \qquad m \downarrow 1 \tag{1.2.23}$$

$$P_a(t) \sim t^{-\frac{1}{\gamma-2}} \qquad t \to \infty \tag{1.2.24}$$

$$\mu(t) \equiv 1 \tag{1.2.25}$$

$$\mu(t|dT) \sim T^{\frac{1}{\gamma-2}} \frac{t}{T}\Big(1 - \frac{t}{T}\Big)^{\frac{1}{\gamma-2}} \qquad T \to \infty,\ t/T \text{ finite} \tag{1.2.26}$$

The critical behaviours described above may be perceived as of a non-standard mean-field theory and this class of irregular BP is suitable to model avalanches with intense fluctuations even when all the dynamical correlations are ignored.

It is also worth mentioning that for BP with divergent offspring number variance, in the subcritical regime away from criticality, the avalanche size distribution may still manifest power-law in a certain range [29], a phenomenon uncharacteristic of regular BP. This is one of the examples where power-law statistics of a key observable does not guarantee criticality of the dynamics, which one should bear in mind when modelling complex systems.

### 1.2.2 Inhomogeneous Markov BP

As stated at the beginning of **subsection 1.2.1**, Markovianity of BP means that at any given time $t$, all the existing particles are subject to the same *global* branching rate and mechanism, hence memoryless as the process of population size. Inhomogeneity however, suggests that the global branching rate and mechanism may vary, deterministically or stochastically, with environment (additional degrees of freedom) or over time. Here we give a brief discussion on the simple cases of Markov BP with branching rate and/or branching mechanism deterministically varying over time.

For Markov BP with time-dependent branching rate $r(t)$ and branching mechanism $f(z,t)$, the master equation Eq.(1.2.1) still holds, hence the forward Kolmogorov equation Eq.(1.2.2) is transformed into

$$\begin{aligned} &\frac{\partial F}{\partial t} = r(t)\frac{\partial F}{\partial z}[f(z,t)-z] \\ &F(z,0) = z \end{aligned} \tag{1.2.27}$$

When only the branching rate is time-dependent and the branching mechanism fixed, we can separate variables for $F(z,t)$ and solve Eq.(1.2.27) by the method of characteristics the same way as for Eq.(1.2.2). The solution would simply be replacing $rt$ in the solution of Eq.(1.2.2) with $\int_0^t r(t')dt'$, where the time-dependent branching rate serves as a non-uniform rescaling of time. This means that Eq.(1.2.4) also holds after a change of time variable, hence Theorem 1 and 2 follow. In terms of critical behaviours, $\beta' = 1$ and $\theta = 0$ follow from Eq.(1.2.7) and Eq.(1.2.11) unchanged, while $\delta$ from Eq.(1.2.10) depends on the particular form of $r(t)$ as

$$P_a(t) \sim \frac{1}{\int_0^t r(t')dt'} \qquad t \to \infty \tag{1.2.28}$$

When the branching mechanism is time-dependent, the situation is more complicated. In general, the BP would still exhibit an absorbing phase tran-

sition, but even the criticality of the APT depends on the specific form of $f(z,t)$. In some applications, however, the time-dependence of $f(z,t)$ can be treated as perturbation, then similar techniques for the analysis of homogeneous Markov BP can be applied to calculate observables near or at the criticality of the unperturbed BP.

### 1.2.3 Age-dependent BP

When we loosen the constraint of Markovianity, existing particles of BP may be subject to different branching rates or branching mechanisms. One of the most widely studied and applied classes of non-Markovian BP is the so-called *age-dependent* BP [32, 23]. Consider a single type branching particle system [38] where newborn particles are subject to the same law: a general life-time distribution $G(t)$ and age-dependent regular branching mechanisms $f(z,t) := \mathbb{E}[z^{K(t)}]$, where $K(t)$ is the offspring number of a particle branching at age $t$ with probability mass function (distribution) $\{p_k(t)\}_{k=0,1,\dots}$ and $f(\bullet,t)$ analytic in $[0,1]$ for all $t \geqslant 0$. The BP initiates with one newborn particle[1], $N(0) = 1$. Although $\{N(t)\}_{t\geqslant 0}$ is non-Markovian and the master equation doesn't hold, the process is renewal at the first branching event and its generating function $F(z,t)$ satisfies a renewal equation adapted from Eq.(1.2.4):

$$\begin{aligned} F(z,t) &= z[1-G(t)] + \int_0^t dG(t_1) f[F(z,t-t_1),t_1] \qquad (1.2.29)\\ F(z,0) &= z. \end{aligned}$$

Intuitively the first item on the right hand side of Eq.(1.2.29) accounts for the initial particle not branching by $t$ and the second item the first branching occurring at $t_1 \in (0,t)$ with branching mechanism $f(\bullet,t_1)$. When the branching mechanism is fixed $f(z,\cdot) \equiv f(z)$ and only the branching rate is age-dependent, the process reduces to a Bellman-Harris BP [32].

[1] BP with different initial conditions can be easily characterised with the simplest situation discussed here as building block.

• **Survival probabilities $P_a^*$ and $P_a(t)$**

Denote finite-time and eventual extinction probabilities as $Q(t) := F(0,t)$ and $q := Q(\infty)$, same as in previous sections. Let $z = 0$ in Eq.(1.2.29) we have

$$Q(t) = \int_0^t dG(t_1) f[Q(t-t_1), t_1] \tag{1.2.30}$$

Take $t \to \infty$ on both sides of Eq.(1.2.30), the limit is allowed also in the integrand given the fact that $0 \leqslant Q(\cdot) \leqslant 1$ and $0 \leqslant f[Q(\cdot), \cdot] \leqslant 1$. Hence

$$q = \int_0^\infty dG(t_1) f[q, t_1] \tag{1.2.31}$$

Further define $\bar{\bar{f}}(z) := \int_0^\infty dG(u) f(z,u)$. It is easy to see that $\bar{\bar{f}}(1) = 1$, $\bar{\bar{f}}(z)$ is monotonically increasing and inherits the basic properties of $f(z,\cdot)$ (e.g., convexity, analyticity). Eq(1.2.31) can then be rewritten as

$$q = \bar{\bar{f}}(q), \tag{1.2.32}$$

and we have analogous to Theorem 1:

**Theorem 3.** (i) *$q$ is the smallest root of $\bar{\bar{f}}(z) = z$ in $[0,1]$, which exists.*
(ii) *Denote $\bar{\bar{m}} := \bar{\bar{f}}'(1)$. If $\bar{\bar{m}} > 1$, then $q < 1$; Otherwise $q = 1$.*
*Age-dependent BP with $\bar{\bar{m}}$ ><= 1 are referred to as super-, sub-, critical respectively.*

with $\bar{\bar{f}}(z)$ playing the role of effective branching mechanism. Since $\bar{\bar{f}}(z)$ is analytic, we immediately have

$$P_a^* = 1 - q \sim |\bar{\bar{m}} - 1|, \qquad \bar{\bar{m}} \downarrow 1, \tag{1.2.33}$$

same as in the Markovian case with the standard mean-field exponent $\beta' = 1$.

To obtain the asymptotic behaviour of $Q(t)$ (hence $P_a(t)$) from Eq.(1.2.30) takes a little more effort. Here we summarise part of the results from [39, 40]:

**Theorem 4.** (i) *Define $I_{i,j} := \int_0^\infty u^i \partial_z^j f(1,u) dG(u)$.*
*If $I_{0,1} = \int_0^\infty \partial_z f(1,u) dG(u) = 1$ and $I_{0,2} > 0$ (non-trivial condition), the*

*age-dependent BP is critical. If further $I_{0,3}$, $I_{3,0}$ and $I_{3,3}$ are all finite, (which implies that $I_{i,j}$ are all finite for $0 \leqslant i, j \leqslant 3$), then*

$$P_a(t) = 1 - Q(t) \simeq \frac{2I_{1,1}}{I_{0,2}\, t}, \qquad t \to \infty \tag{1.2.34}$$

(ii) *In the Bellman-Harris case, the constraints can be loosened to second moments of the life-time distribution. If $m = f'(1) = 1$, $0 < m_2 = f''(1) < \infty$, $\bar{t} = \int_0^\infty t\, dG(t) < \infty$ and $t^2[1 - G(t)] \to 0$ as $t \to \infty$, then Eq.(1.2.34) holds in the new notations*

$$P_a(t) \simeq \frac{2\bar{t}}{m_2 t}, \qquad t \to \infty \tag{1.2.35}$$

In short, when $G(t)$ is relatively "well-behaved", we recover the standard mean-field exponent $\delta = 1$.

For the critical behaviours of $\mu(t)$ and $\mu(t|dT)$, we can make use of the following renewal theorems [23, p144-145]:

**Theorem 5.** (i) *Define the renewal function*

$$U_\alpha(t) := \sum_{n=0}^{\infty} \alpha^n G^{*n}(t), \qquad t \geqslant 0 \tag{1.2.36}$$

*where $G$ is a distribution function on $[0, \infty)$, $G^{*n}$ its $n$-fold convolution with $G^{*0} \equiv 1$ and $0 < \alpha < \infty$ a constant. It solves the integral equation*

$$U_\alpha(t) = 1 + \alpha \int_0^t U_\alpha(t - u) dG(u), \qquad t \geqslant 0 \tag{1.2.37}$$

(ii) *Integral equation*

$$H(t) = \zeta(t) + \alpha \int_0^t H(t - u) dG(u), \qquad t \geqslant 0 \tag{1.2.38}$$

*where $\zeta(t)$ is a bounded measurable function on $[0,\infty)$ has the unique solution*

$$H(t) = (\zeta * U_\alpha)(t) := \int_0^t \zeta(t-u) dU_\alpha(u) \tag{1.2.39}$$

*which is bounded on finite intervals.*

**Theorem 6.** *Define $\bar{t} := \int_0^\infty t dG(t) \leqslant \infty$ and other notations follow from Theorem 5. Let $\alpha = 1$.*
(i) *If $\zeta_0 := \lim_{t\to\infty} \zeta(t)$ exists, then $\lim_{t\to\infty} H(t)/t = \zeta_0/\bar{t}$.*
(ii) *If $\zeta(t)$ is Riemann integrable, then $\lim_{t\to\infty} H(t) = [\int_0^\infty \zeta(u)du]/\bar{t} = \text{const.}$*

• **Population size evolution** $\mu(t)$
From Eq.(1.2.29) we have

$$\mu(t) = 1 - G(t) + \int_0^t dG(t_1)\partial_z f(1,t_1)\mu(t-t_1) \tag{1.2.40}$$

Define $\overline{G}(t) := 1 - G(t)$ and $\bar{\bar{G}}(t) := \int_0^t dG(u)\partial_z f(1,u)$. Since at criticality

$$\int_0^\infty dG(u)\partial_z f(1,u) = \bar{\bar{f}}'(1) = 1, \tag{1.2.41}$$

$\bar{\bar{G}}(t)$ can serve as the effective life-time distribution with $\bar{\bar{G}}(0) = 0$ and $\bar{\bar{G}}(\infty) = 1$. Eq.(1.2.40) can be rewritten as

$$\mu(t) = \overline{G}(t) + \int_0^t d\bar{\bar{G}}(u)\mu(t-u), \tag{1.2.40}$$

thus according to Theorem 5, has solution

$$\mu(t) = (\overline{G} * \bar{\bar{U}})(t) \tag{1.2.43}$$

where $\bar{\bar{U}}(t) := \sum_{n=0}^\infty \bar{\bar{G}}^{*n}(t)$.

In the case of Bellman-Harris, $\bar{\bar{G}}(t) = G(t)$, it is easy to verify that $\mu(t) \equiv 1$ is the solution of Eq.(1.2.40), and the standard mean-field exponent $\theta = 0$ follows. The general asymptotic behaviour of $\mu(t)$ at large $t$ may depend

on the forms of $G(t)$ and $\bar{\bar{G}}(t)$. Since $\overline{G}(\infty) = 0$, from Theorem 6(i) we have $\lim_{t\to\infty} \mu(t)/t = 0$, $\mu(t) \sim o(t)$ at large $t$, hence $\theta < 1$. Further if $\overline{G}(t)$ is Riemann integrable (which can be ensured if $\lim_{t\to\infty} t^2\overline{G}(t) = 0$), then from Theorem 5(ii), we again have $\theta = 0$. If however, $\overline{G}(t)$ decays slow enough, it is possible to construct a critical age-dependent BP with sublinearly growing population and exponent $0 < \theta < 1$ deviating from the standard mean-field value.

• **Temporal profile** $\mu(t|dT)$

For simplicity, we restrict our attention to the Bellman-Harris case. Following the notations in **subsubsection 1.2.1.1**, we derive the renewal equation by conditioning the branching time of the initial particle $\tau_1$ at $t_1 \in [t, T)$ or $t_1 \in [0, t)$.

$$\begin{aligned}
P(n,t|T) =& \frac{1}{Q(T)}\mathbb{P}\{N(t) = n, N(T) = 0|N(0) = 1\} \\
=& \frac{1}{Q(T)}\Bigg[\delta_{n,1}\mathbb{P}\{\tau_1 > t, N(T) = 0|N(0) = 1\} \\
&+ \int_0^t \mathbb{P}\{\tau_1 \in dt_1\}\sum_k p_k \mathbb{P}\{N(t) = n, N(T) = 0|N(t_1) = k\}\Bigg] \\
=& \frac{1}{Q(T)}\Bigg[\delta_{n,1}\int_t^T dG(t_1)\sum_k p_k Q^k(T - t_1) \\
&+ \int_0^t dG(t_1)\sum_k p_k Q^k(T - t_1)P^{*k}(n, t - t_1|T - t_1)\Bigg] \qquad (1.2.44)
\end{aligned}$$

Define $\tilde{F}(z,t|T) := Q(T)F(z,t|T)$ and $\tilde{\mu}(t|T) := Q(T)\mu(t|T)$, we have

$$\tilde{F}(z,t|T) = z\int_t^T dG(t_1)f[Q(T - t_1)] + \int_0^t dG(t_1)f[\tilde{F}(z, t - t_1|T - t_1)] \qquad (1.2.45)$$

and

$$\tilde{\mu}(t|T) = \int_t^T dG(t_1) f[Q(T-t_1)] + \int_0^t dG(t_1) f'[Q(T-t_1)] \tilde{\mu}(t-t_1|T-t_1) \tag{1.2.46}$$

The first item on the right hand side of Eq.(1.2.46) can be expressed as

$$\xi(t,T) := \int_t^T dG(t_1) f[Q(T-t_1)] = \int_0^{T-t} du G'(t+u) f\big[Q(T-t-u)\big] \tag{1.2.47}$$

by changing of variable $t_1 = t+u$. If the life-time distribution $G(t)$ has exponential tail, i.e.,

$$\overline{G}(t) = 1 - G(t) \simeq e^{-\tilde{r}t}, \qquad t \to \infty \tag{1.2.48}$$

where $0 < \tilde{r} < \infty$ is the asymptotic hazard (branching) rate, we have

$$G'(t+u) \simeq \overline{G}(t) G'(u), \qquad t, u \to \infty \tag{1.2.49}$$

Since we are interested in the asymptotic behaviour of the solution at $t, T \to \infty$ and $t/T$ finite, plug Eq.(1.2.49) into Eq.(1.2.47) we get

$$\xi(t,T) \simeq \overline{G}(t) \int_0^{T-t} du G'(u) f[Q(T-t-u)] = \overline{G}(t) Q(T-t). \tag{1.2.50}$$

The last equality is due to the fact that $Q(T-t) = \int_0^{T-t} du G'(u) f[Q(T-t-u)]$, which can be obtained from Eq.(1.2.45) by setting $z = 1$ and $T \leftarrow T-t$.

With approximation Eq.(1.2.50), the renewal equation Eq.(1.2.46) turns into

$$\tilde{\mu}(t|T) \doteq \overline{G}(t) Q(T-t) + \int_0^t dG(t_1) f'[Q(T-t_1)] \tilde{\mu}(t-t_1|T-t_1) \tag{1.2.51}$$

Notice that this is of the same form as the renewal equation in the Markovian case, where the BP being extinct by $T$ conditioned on no branching by $t$ is

equivalent to the BP being extinct by $(T-t)$ (from one initial particle). Eq.(1.2.51) is solved by

$$\tilde{\mu}(t|T) \doteq Q(T-t)\frac{Q'(T)}{Q'(T-t)}, \tag{1.2.52}$$

equivalent to the Markovian solution of $\mu(t|T)$ in Eq.(1.2.18). This can also be verified directly by utilising the Markovian renewal equation of finite-time extinction probability

$$Q(T) = \overline{G}(t)Q(T-t) + \int_0^t dG(t_1)f[Q(T-t_1)]. \tag{1.2.53}$$

From Eq.(1.2.52) we can extract the temporal profile, which naturally takes the same form as Eq.(1.2.19):

$$\mu(t|dT) = 1 + \frac{Q(T-t)}{Q'(T)}\frac{d}{dT}\left[\frac{Q'(T)}{Q'(T-t)}\right] \tag{1.2.53}$$

Since for Bellman-Harris BP, the asymptotic behaviour of $Q(t)$ also coincides with the Markovian case, we conclude that the temporal profiles of Bellman-Harris BP with life-time distribution adopting exponential tail scale exactly the same as those of homogeneous Markov BP:

$$\mu(t|dT) \sim T\frac{t}{T}(1-\frac{t}{T}), \qquad T\to\infty,\ t/T \text{ finite} \tag{1.2.54}$$

with the parabolic avalanche shape. This is a major original result of this chapter, which proves the conjecture proposed in [27] based on numerical simulations, that the temporal profiles of age-dependent BP show transient non-universal behaviours for small $t$ and resume the universal behaviour of its Markovian counterpart for large $t$.

Finally, it's worth mentioning that for age-dependent BP, when the life-time distribution $G(t)$ belongs to the so-called *sub-exponential* class, $\mu(t)$

and $P_a(t)$ may admit algebraic asymptotic behaviours for large $t$ in the sub-critical regime [23, p152,p168], which in turn leads to power-law avalanche size distributions. This is the second scenario that we encounter (after the one mentioned at the end of **subsubsection 1.2.1.2**) in BP with essential observables demonstrating power-law off criticality.

### 1.2.4 BP with immigration

We conclude our survey of the critical behaviours of BP with another widely considered set-up: BP with immigration [23, 41, 33]. In the terms of reacting particle systems, this corresponds to particle creation from external sources, and once created (join the system) particles are subject to the same law of BP independently.

When immigration is allowed, the system formally no longer admits an absorbing state. In order to be put in touch with avalanche dynamics, one should consider slow immigration rate and population processes separated by the zero state as avalanches. The exact probabilistic model, i.e., continuous-time BP with one initial particle and immigration stopped at the zero population state, turns out to be challenging[2]. In this set-up, upon first branching the system is no longer renewal (consisting of independently evolving subsystems), since the families of the first generation of offspring collectively but asynchronously affect potential immigration, which also composes part of the system.

On the other hand, a coarse-grained approach may help to bypass the technical difficulties, as is adopted in [42]. Consider the population process $\{N(t)\}$ rescaled by a large parameter $\Omega$, the resulted process $\rho(t) := N(t)/\Omega$ can be treated as a continuous state stochastic process initiated at $\rho(0) = 0^+$. For simplicity, assume the original BP is Markovian and homogeneous, with branching rate $r = 1$ and regular branching mechanism $f(z)$. Denote $m =$

[2] To our best knowledge still open question.

$f'(1)$, $m_2 = f''(1)$ and $\epsilon = 1 - m$, then the population "field" $\rho(t)$ satisfies the Langevin equation with multiplicative noise:

$$\frac{d}{dt}\rho = -\epsilon\rho + \sqrt{\rho}\xi(t) \tag{1.2.55}$$

where $\langle \xi(t)\xi(t')\rangle = 2m_{\cdot}\delta(t-t')$ and . As pointed out in [42], Eq.(1.2.55) should be understood in the *Ito* sense to be consistent with the absorbing state at 0, and may also be referred to as a *demographic random walk*. To incorporate a slow immigration rate $h$ in the original BP would simply mean adding an external field $h$ to the right hand side of Eq.(1.2.55):

$$\frac{d}{dt}\rho = h - \epsilon\rho + \sqrt{\rho}\xi(t) \tag{1.2.56}$$

Following the procedure in [42], Eq.(1.2.56) can be rewritten in the *Stratonovich* sense and transformed to an equation describing a one-dimensional random walk in a logarithmic potential:

$$\mathring{x} = \frac{2h - m_2}{4x} - \frac{\epsilon}{2}x + \eta(t) \tag{1.2.57}$$

where $\mathring{x}$ stands for the time derivative in the Stratonovich sense and $\langle \eta(t)\eta(t')\rangle = \frac{m_2}{2}\delta(t-t')$. For $x(0) = 0^+$, the first return time of the random walk is identified as avalanche duration. Let $\epsilon = 0$ (the underlying BP critical), one can derive the first return time distribution from Eq.(1.2.57), and together with the scaling argument $\rho \sim \sqrt{\rho}\sqrt{t}$, fully characterise the (coarse-grained) avalanche statistics. The exponents are given as [42]

$$\tau_{\text{T}} = 2 - h/m_2, \qquad \gamma_{\text{ST}} = 2 \tag{1.2.58}$$

From scaling laws Eq.(1.1.9) and Eq.(1.1.11), we thus have

$$\delta = 1 - h/m_2, \qquad \theta = h/m_2 \tag{1.2.59}$$

Since BP with slow immigration stopped at zero is critical (in terms of APT) when the underlying BP is critical, Eq.(1.2.59) gives the dynamical expo-

nents of at criticality of a non-interacting particle system different from the standard mean-field values. It is interesting to note that these exponents depend on the immigration rate $h$ thus are continuously tunable. One may come to terms with these behaviours by viewing an avalanche in this scenario as the composition of sub-avalanches initiated at different times.

## 1.3 Summary Remarks

In this chapter, we first introduce the concepts of absorbing phase transitions (APT) and how their dynamical critical behaviours are linked to characterisation of critical avalanches, laying the foundation for our main interest in the studies of stochastic particle systems throughout this thesis. Then we focus on non-spatial branching processes (BP), the simplest family of particle systems admitting APT and prototypical candidates of mean-field theories (MFT). Most of the results presented here are not original, the main purpose is to examine a few most important classes of BP from the lens of APT and critical avalanches and reveal the universality of mean-field critical behaviours from an approach mathematically as unified as possible. We see that the standard mean-field universality class which is often associated with all BP by default in physics literatures arises from the homogeneous Markovian and regular case, and is largely robust as long as the branching mechanism is fixed and regular, including for BP with time-dependent branching rates and non-Markovian Bellman-Harris BP. With irregular or varying branching mechanism, critical behaviours may deviate from the standard mean-field results, although they can still be considered as MFT due to the additive independence nature of branching particle systems, and treated consistently by the Markovian master equation or the renewal integral equation of the generating function. Some of the derivations and comments are published as [25], and the results about the temporal profiles of Bellman-Harris BP are fresh.

We also note that power-law/algebraic scaling of key observables may present in non-critical regimes, phenomena which often come up in the discussions of controversies regarding critical avalanches of complex systems [43, 44, 28, 45, 24, 29].

# 2

# Absorbing Phase Transitions and Finite-Time Properties of Spatial Branching Processes

Complex systems with APT and critical avalanches usually involve spatial degrees of freedom. To see how the spatial factor features in these phenomena in a minimalistic fashion, we again consider branching particle systems which are absent of all (explicit) dynamical correlations and the models of mean-field approximation for interacting particle systems.

Spatial BP, including branching random walks (BRW) and branching diffusions, incorporate salient phenomenology and are of both theoretical and applicational importance. They have been extensively studied in recent years by both mathematicians and physicists and remain active topic for both communities. Just to name a few fruitful directions of late: In bounded domains, "pure" branching generates spatial correlations which typically leads to clus-

tering of the population, phenomena which are of significance in modelling ecological systems and neutron reactions [46, 47, 48, 49]; In open domains, the propagation of travelling waves or the extreme values of spatial BP are highly important mathematical objects [50, 51, 52], apart from their wide applications in population ecology [53] / genetics [54] and epidemics [55].

Here, we limit our attention to the evolution of population size of spatial BP, which differs from that of non-spatial BP only in terms of boundary effects to the population size. The purpose of this chapter is two-fold: Firstly, to provide a more comprehensive understanding of the critical behaviours of branching particle systems as the extension of **Chapter 1**; And secondly, to introduce the powerful iteration method for approximating the solutions of renewal equations originated from BP, spatial or non-spatial. The method is frequently seen in the proofs of the theory of BP [23, 41]. Nonetheless, we put an emphasis on its physical interpretation and its effectiveness in modelling complex systems, illustrated by a new application with our recurring interest in critical avalanches: the temporal profiles of branching diffusion.

## 2.1 Some Results and Remarks on APT of Spatial BP

### 2.1.1 Branching diffusions in bounded domains

Consider a spatial BP in a bounded domain with absorbing (Dirichlet) boundary conditions, i.e., particles killed at boundaries or regarded as leaving the system. For simplicity, the underlying BP is homogeneous Markovian and regular. In additional, particles are independently subject to Markovian diffusion, with generator (operator) $\hat{L}$. The spatial BP is clearly Markovian in terms of the evolution of particle configuration or particle density distribution, but generally non-Markovian for the population size evolution. Initiated from one particle at arbitrary location, under mild boundary geometric constraints (Lipschitz boundaries), the spatial BP admits a continuous APT at

the critical point of $r(m-1) = \lambda_1$, where $r$ is the branching rate, $m$ the mean offspring number of BP, and $\lambda_1$ the first (smallest) eigenvalue of $\hat{L}$ under prescribed boundary conditions [56]. Above or below the critical point, the expected population size grows or decays exponentially, while keeps constant at criticality, a direct consequence of the so-called "many-to-one" lemma [57]. [56] also found that at criticality, the finite-time extinction probability algebraically decays as $t^{-1}$. Hence $\theta = 0$, $\delta = 1$.

Since the critical condition is given by a combination of parameters characterising branching and diffusion, there are a number of ways to approach criticality. For a bounded domain in one dimension, [58] found that $\beta' = 1$ if one approach the critical domain size from above. It is easy to see that the exponent doesn't change if approaching from the BP parameters (linear critical condition).

The key reason for the above spatial BP to exhibit standard mean-field critical behaviours lies in the spectral theory of the diffusion operator. For Dirichlet boundary conditions in bounded domains, one expects a separation of spatial and temporal variables, and a discrete spectrum with the smallest eigenvalue governing the survival rate (from exiting the domain) of diffusive particles. The competition of pure branching and killing at the boundary, both exponential with respect to time, determine the critical point and necessarily belonging to the standard mean-field universality class. From this argument, we see that pure absorbing boundary conditions can be relaxed to at least partially absorbing (otherwise no difference from the non-spatial case), which could only change the critical point via $\lambda_1$ but not the critical behaviours. If however the diffusion is anomalous, e.g., fractional diffusion [59], we might expect a different universality class.

### 2.1.2 Branching diffusions with drift on the half line

Now consider BP in unbounded space with partially absorbing boundary conditions, the simplest case being on an half line with absorbing boundary at

the origin. Again assume the underlying BP is homogeneous Markovian and regular, and particles are subject to Brownian motion with a negative drift $\hat{L} = \frac{1}{2}\frac{\mathrm{d}}{\mathrm{d}x^2} - v\frac{\mathrm{d}}{\mathrm{d}x}$. At first glance, this process is almost identical with the one limited on bounded domains. Surprisingly, the open geometry plays a crucial part in the "criticality" of the process and completely shifts the landscape.

Early work [60] found that the spatial BP described above admits a continuous APT with respect to the drift $v$ as parameter. If we further set the branching rate at unity and assume that a particle deterministically splits into two per branching, then $v_c = \sqrt{2}$ is the critical point. The particle system, initiated from one at arbitrary position $x_0$, persists with positive probability if $v < v_c$ and perishes almost surely if otherwise, corresponding to active and absorbing phases.

Recent works [61, 62, 63, 64] have characterised the asymptotic behaviours of this process near or at criticality in great details. Here we use the term critical or criticality purely referring to the parameter value at which a phase transition occurs, as in line with the mathematical literatures. We shall see that it does *not* pertain the critical behaviours in the commonly used statistical physics sense.

When the drift $v$ approaches the critical value from below, define $\epsilon = 2 - v^2$. [61] found that the eventual survival probability follows

$$P_a^* \sim \epsilon^{-1/2} e^{\sqrt{2}\pi\epsilon^{-1/2}} \tag{2.1.1}$$

Although with an algebraic component, Eq.(2.1.1) is quite different from the scaling behaviours in the theory of critical phenomena in statistical physics, since the exponential part dominates the decay as $\epsilon \downarrow 0$. In a sense, this means the typical time-scale not only doesn't diverge but in fact vanishes approaching the critical point.

For the finite-time survival probability at criticality, [63] found that

$$P_a(t) \sim e^{-(3\pi^2 t)^{1/3}} \tag{2.1.2}$$

Again this is unusual for "critical" behaviours, as the survival probability decays faster than any power-law would predict.

Now we should expect the evolution of population size not to scale as a constant, which is indeed the case as shown in [64].

In short, the scaling ansatz and therefore the scaling exponents introduced in **section 1.1** are not suitable to characterise the spatial BP here, a reminder that we should not expect to transplant the paradigms of heuristic physical arguments without scrutiny.

## 2.2 Finite-Time Properties of Spatial BP

The results discussed above, i.e., critical behaviours of spatial BP, are for large $t$ asymptotics. In applications, either as model of population dynamics or approximation of some interacting particle systems, one might be interested in observables of spatial BP in finite time comparable to the average branching waiting time. For this purpose, we introduce the iteration method which is highly flexible for renewal equations stemming from BP. We illustrate the method in an example of spatial BP, but similar techniques can be easily translated to other set-ups, including almost all of the examples considered in **Chapter 1**.

We elaborate and slightly generalise the set-up adopted in [56]. Consider a branching diffusion in a bounded domain $\Omega$ satisfying Lipschitz conditions and having at least partially absorbing boundary conditions. Let $\hat{L}$ be the generator of diffusion on $\Omega$ with the first eigenvalue $\lambda_1$. The probability density of a simple (non-branching) diffusive particle initially placed at $\mathbf{x}$ to be at $\mathbf{y}$ at time $t$ is $p(\mathbf{y}, \mathbf{x}; t) = g(\mathbf{y}, t|\mathbf{x}, 0)$, where $g(\mathbf{y}, t|\mathbf{x}, t')$ is the Green function of the diffusion, i.e.,

$$(\partial_t - \hat{L}_{\mathbf{y}})g(\mathbf{y}, t|\mathbf{x}, t') = \delta(\mathbf{y} - \mathbf{x})\delta(t - t') \tag{2.2.1}$$

The survival probability of a simple particle initially placed at $\mathbf{x}$ by time $t$ is

then

$$p_a(\mathbf{x},t) := \int_\Omega d\mathbf{y} p(\mathbf{y},\mathbf{x};t) \tag{2.2.2}$$

and the complement extinction probability $\overline{p}_a(\mathbf{x},t) := 1 - p_a(\mathbf{x},t)$.
Note that for all $t' \in (0,t)$,

$$\begin{aligned} & p(\mathbf{y},\mathbf{x};t) = \int_\Omega d\mathbf{x}' p(\mathbf{x}',\mathbf{x};t') p(\mathbf{y},\mathbf{x}';t-t') \\ \Longrightarrow \quad & p_a(\mathbf{x},t) = \int_\Omega d\mathbf{x}' p(\mathbf{x}',\mathbf{x};t') p_a(\mathbf{x}',t-t') \end{aligned} \tag{2.2.3}$$

Assume branching is time-homogeneous with general life-time distribution $G(t)$ and regular branching mechanism $f(\cdot)$ with mean offspring number $m := f'(1)$. Denote $\overline{G}(t) := 1 - G(t)$, thus the maximum branching rate is given by $r_1 := \max_{t \geqslant 0} \{G'(t)/\overline{G}(t)\}$. To impose that $m \leqslant 1 + \lambda_1/r_1$ would ensure the branching diffusion being subcritical or critical.[1]

Let $N_{\mathbf{x}}(t)$ be number of particles at time $t$ for the branching diffusion started with one particle at $\mathbf{x}$. Then

$$\begin{aligned} \mathbb{P}\{N_{\mathbf{x}}(t) = n\} = & \overline{G}(t)\left[\delta_{n0}\overline{p}_a(\mathbf{x},t) + \delta_{n1} p_a(\mathbf{x},t)\right] + \int_0^t dG(t_1) \\ & \cdot \left[\delta_{n0}\overline{p}_a(\mathbf{x},t_1) + \int_\Omega p(d\mathbf{y},\mathbf{x};t_1) \sum_k p_k \mathbb{P}^{*k}\{N_{\mathbf{y}}(t-t_1) = n\}\right] \end{aligned} \tag{2.2.4}$$

where the first term on the right hand side accounts for the first branching time $\tau_1 > t$ and the initial particle absorbed at the boundaries or remaining, and the second term conditions on $\tau_1 = t_1 < t$ and branching position at $\mathbf{y}$

[1] This condition ensures the convergence of the iteration schemes which we give later; But if only a few iterations are necessary to give good approximation for practical consideration, the condition can be lifted.

if not absorbed by time $t_1$. The generating function of $N_{\mathbf{x}}(t)$ follows

$$F_{\mathbf{x}}(z,t) = \overline{G}(t)\left[\overline{p}_a(\mathbf{x},t) + zp_a(\mathbf{x},t)\right] + \int_0^t dG(t_1) \cdot \left[\overline{p}_a(\mathbf{x},t_1) + \int_\Omega p(d\mathbf{y},\mathbf{x};t_1) f\left[F_{\mathbf{y}}(z,t-t_1)\right]\right] \tag{2.2.5}$$

• Finite-time extinction probability $Q_{\mathbf{x}}(t) := F_{\mathbf{x}}(0,t)$ follows

$$Q_{\mathbf{x}}(t) = \overline{G}(t)\overline{p}_a(\mathbf{x},t) + \int_0^t dG(t_1)\left[\overline{p}_a(\mathbf{x},t) + \int_\Omega p(d\mathbf{y},\mathbf{x};t) f\left[Q_{\mathbf{y}}(t-t_1)\right]\right] \tag{2.2.6}$$

• Expected population size evolution $\mu_{\mathbf{x}}(t) := \langle N_{\mathbf{x}}(t)\rangle = F'_{\mathbf{x}}(1,t)$ follows

$$\mu_{\mathbf{x}}(t) = \overline{G}(t)p_a(\mathbf{x},t) + m\int_0^t dG(t')\int_\Omega p(d\mathbf{y},\mathbf{x};t')\mu_{\mathbf{y}}(t-t') \tag{2.2.7}$$

If branching is Markov with rate $r$, then $G(t) = 1 - e^{-rt}$, the linear integral equation Eq.(2.2.7) is solved by

$$\mu_{\mathbf{x}}(t) = e^{r(m-1)t}p_a(\mathbf{x},t), \tag{2.2.8}$$

which is easily verifiable by utilising the transitive property Eq.(2.2.3). This is the many-to-one lemma [51, 62, 57] in probability literatures, which can be interpreted as: The expected population size of the branching diffusion at time $t$ is the expected number of particles produced by the underlying BP times the survival probability of a simple diffusive particle; Each leaf in the genealogical tree of BP (up to time $t$) contributes equally to the expected population size with the weight of the probability of remaining in the domain, a direct consequence of additive independence of branching diffusions.

Similarly, denote $F_{\mathbf{x}}(z,t|dT) := \mathbb{E}[z^{N_{\mathbf{x}}(t|dT)}]$, $F_{\mathbf{x}}(z,t|T) := \mathbb{E}[z^{N_{\mathbf{x}}(t|T)}]$ and

$\tilde{F}_{\mathbf{x}}(z,t|T) := Q_{\mathbf{x}}(t)F_{\mathbf{x}}(z,t|T)$, then

$$\begin{aligned}\tilde{F}_{\mathbf{x}}(z,t|T) =& \sum_n z^n \mathbb{P}\{N_{\mathbf{x}}(t)=n, N_{\mathbf{x}}(T)=0\} \\ =& \overline{G}(t)\left[\bar{p}_a(\mathbf{x},t) + z\int_\Omega p(d\mathbf{y},\mathbf{x};t)Q_{\mathbf{y}}(T-t)\right] \\ &+ \int_0^t dG(t_1)\left[\overline{p}_a(\mathbf{x},t) + \int_\Omega p(d\mathbf{y},\mathbf{x};t_1) f\left[\tilde{F}_{\mathbf{y}}(z,t-t_1|T-t_1)\right]\right]\end{aligned} \tag{2.2.9}$$

• Temporal profile $\mu_{\mathbf{x}}(t|dT)$ and cumulated temporal profile $\mu_{\mathbf{x}}(t|T)$ can be obtained from $\tilde{\mu}_{\mathbf{x}}(t|T) := Q_{\mathbf{x}}(t)\mu_{\mathbf{x}}(t|T)$ which follows

$$\begin{aligned}\tilde{\mu}_{\mathbf{x}}(t|T) =& \overline{G}(t)\int_\Omega p(d\mathbf{y},\mathbf{x};t)Q_{\mathbf{y}}(T-t) + \int_0^t dG(t_1) \\ &\cdot \int_\Omega p(d\mathbf{y},\mathbf{x};t_1) f'\left[Q_{\mathbf{y}}(T-t_1)\right]\tilde{\mu}_{\mathbf{y}}(t-t_1|T-t_1)\end{aligned} \tag{2.2.10}$$

Define $\zeta_{\mathbf{x}}(t,T) := \overline{G}(t)\int_\Omega p(d\mathbf{y},\mathbf{x};t)Q_{\mathbf{y}}(T-t)$, the above equation can be solved by iteration:

$$\begin{aligned}&\tilde{\mu}_{\mathbf{x}}^{(0)}(t|T) = \zeta_{\mathbf{x}}(t,T) \\ &\tilde{\mu}_{\mathbf{x}}^{(i+1)}(t|T) = \zeta_{\mathbf{x}}(t,T) + \int_0^t dG(t_1)\int_\Omega p(d\mathbf{y},\mathbf{x};t_1) f'[Q_{\mathbf{y}}(T-t_1)]\tilde{\mu}_{\mathbf{y}}^{(i)}(t-t_1|T-t_1) \\ &i = 0,1,\ldots\end{aligned} \tag{2.2.11}$$

Clearly $\tilde{\mu}_{\mathbf{x}}^{(i)}(t|T)$ is non-decreasing in $i$; Since $f'\left[Q_{\mathbf{y}}(T-t_1)\right] \leqslant m$ and $\int_\Omega p(\mathbf{y},\mathbf{x};t_1) \leqslant 1$, the iteration limit is uniformly upper bounded according to the renewal theory. Therefore we have uniform convergence

$$\lim_{i\to\infty} \tilde{\mu}_{\mathbf{x}}^{(i)}(t|T) = \tilde{\mu}_{\mathbf{x}}(t|T) \qquad \forall \mathbf{x}\in\Omega,\ 0 \leqslant t \leqslant T \tag{2.2.12}$$

The iteration method described above is versatile and computationally efficient compared to Monte Carlo simulations, since in a few iterations one obtains the desired profile in its entirety. The method also enjoys a nat-

ural physical interpretation, that the $i$-th iteration takes into account the contributions of branching events up to $i$ generations.

# 3

# Multi-Type Branching Process as Effective Mean-Field Theory of Abelian Manna Model

This chapter is based on the paper [65] "*Critical Density of the Abelian Manna model via a multi-type branching process*", Physical Review E 100.3 (2019): 032116, by Nanxin Wei and Gunnar Pruessner.
NW devised the theory, made the analytical calculations, conducted the simulations and produced Figure 3.3, and contributed partially to the manuscript; GP contributed heavily to the manuscript, including the rest of the graphics. The chapter contains large chunks of **verbatim** reproduction of [65] without citation. All other citations follow standard protocols.

In the previous chapters we study in length (spatial) BP with single type of particles which can be perceived as avalanche dynamics, and focus on properties at/near criticality. As mentioned before, the critical behaviour of avalanches is the signature of SOC, which in the mean-field sense can be modelled by BP. For some important feature of SOC models, especially in low dimensions, the plain MFT result may be less than satisfactory. In this chapter we present a concrete example of incorporating short-range dynamical correlations in the multi-type BP as effective MFT, which systematic improves the estimation of the critical point beyond plain MFT.

In the following, we first introduce the Abelian Manna model and its mapping to the multi-type branching process mimicking its avalanche dynamics, then demonstrate how the critical density of AMM can be extracted from the branching process and conclude with a briefdiscussion of the results.

## 3.1 Abelian Manna Model and Self-Organised Branching Process

Manna model [66] is the prototypical stochastic sandpile model proposed for self-organized criticality (SOC) [67]. It was reformulated by Dhar to make it Abelian [68]. The resulting Abelian Manna model (AMM) and its variants have been studied extensively numerically and analytically [69, 70, 71, 72, 73, 74]. Numerical simulations have established that a range of other models belong to the same universality class [21, p. 178], in particular the Oslo Model [75, 76] and the conserved lattice gas [77, 78]. The stationary density of AMM has been estimated with very high precision on hypercubic lattices of dimensions $d = 1$ to $d = 5$ [79, 80, 81, 82, 74]. Yet, theoretical understanding of Manna model is far from complete. In a mean-field theory which ignores all spatial-temporal correlations, the avalanches can be naturally perceived as a binary branching process [83, 84] with branching ratio $\sigma$ twice the particle density $\zeta$ as a mean field. At stationarity, the macroscopic dynamics of driving and dissipation of particles *self-organises* the branching ratio to unity,

which is the critical value, $\sigma_c = 1$, *i.e.* the branching ratio above which a finite fraction of realisations branches indefinitely. The mean-field value of the critical density is therefore $\zeta_{c,(\mathrm{MF})} = \sigma_c/2 = 1/2$ regardless of the dimension of the system [85]. However, numerical findings have placed the critical value $\zeta_c$ of the density clearly above $1/2$ in *any* dimension studied [21, 74], suggesting that the spatial correlations ignored by the mean-field theory are significant.

To facilitate the following discussion, we reproduce the definition of AMM: AMM is normally studied on a $d$-dimensional hypercubic lattice, but extensions to arbitrary graphs are straight forward. Each site carries a non-negative number of particles, which we refer to as the *occupation number*. A site that carries no particle is said to be *empty*, otherwise it is *occupied* by at least one particle. A site carrying less than two particles is *stable*, otherwise it is *active*. If all sites in a lattice are stable, the system is said to be *quiescent*, as it does not evolve by its internal dynamics. If the lattice has $N$ sites, the number of such states is $2^N$. Particles are added to the lattice by an *external drive*. If such an externally added particle arrives at a site that is occupied by a particle already, an avalanche ensues as follows: Every site that carries more than one particle *topples* by moving two of them to randomly and independently chosen nearest neighbours, thereby *charging* them with particles. This might trigger a toppling in turn. The totality of all topplings in response to a single particle added by the external drive is called an avalanche.

We will refer to the evolution from toppling to toppling as the *microscopic time-scale*, as opposed to the macroscopic timescale of the evolution of quiescent states. The evolution from one quiescent state to another quiescent state by adding a particle at a site and letting an avalanche complete is a Markov process. Because of the finiteness of the state space of quiescent configurations and assuming accessibility of all states (but see [74]), the probability to find AMM in a particular quiescent state approaches a unique, stationary, strictly positive value. The analysis below is concerned solely with the the

stationary state of AMM.

For the discussion below we require the notion of occupation number *pre-toppling* and occupation number *post-toppling*. The former refers to the number of particles at a site prior to its possible toppling, the latter refers to the number of particles at a site immediately after possibly shedding (a multiple of) two particles and yet prior to it receiving particles from any other site. Committing a slight abuse of terminology, we will refer to pre- and post-toppling occupation numbers even when the site is stable. Of particular importance to the following consideration is the occupation density $\zeta$, that the expected total number of particles divided by the number of sites.

One paradigm of AMM and SOC in general is the (binary) branching process [32]. The population of that process at any given time is thought to represent those sites that become active as a result of receiving a particle. As they topple, the particles arriving at nearest neighbouring stable sites might activate those, depending on whether they were previously occupied by a particle or not. Any empty site that is charged with only one particle becomes occupied but remains stable. Any stable site charged with two particles is guaranteed to become active. As active sites are sparse, they are rarely charged. However, the Abelian property of AMM means that the arrival of one additional particle at a site leads to a further toppling only if the parity of its occupation number is odd. If two particles arrive at a site, its parity will not change, but the site is bound to topple (once more).

If a neighbouring site becomes active in response to a charge, this corresponds in the branching process to an offspring in the next generation. If two such offspring are generated, this corresponds to a branching that increases the population size. If a neighbouring site turns from empty to occupied, no offspring is produced.

The evolution of an avalanche may thus be thought of as a branching process of activity with strong correlations of branching (doubling) and ex-

tinction events as the lattice occupation dictates whether and where these events take place. Ignoring the lattice and the history of previous and ongoing avalanches, one is left with a plain binary branching process, commonly used to cast AMM and SOC models generally in a mean field theory [85, 14, 86, 87].

In general branching processes, the branching ratio is exactly unity at the critical point of the process, above which the probability of sustaining a finite population size indefinitely is strictly positive. We therefore identify the critical point of the branching process with that of the lattice model.

## 3.2 Self-Organised Multi-Type Branching Process and the Critical Density of AMM

The multi-type branching process considered in the following is based on a mapping of the types of the branching process to the active *motives* of AMM, as shown in Figure 3.1 for the one-dimensional case. These motives indicate the occupation number of the central site pre-toppling (*i.e.* prior to the central site toppling) and the occupation of the neighbouring sites post-toppling (*i.e.* after they may have toppled themselves, which leaves their parity unchanged, but prior to the central site toppling). Defining the motives this way, we can disregard toppling sites charging active neighbouring sites. We effectively keep track only of the change of parity of the neighbouring sites, which is due to charges they receive but does not change when they topple themselves. Within a time step in the multi-type branching process all currently active motives undergo toppling, which corresponds toparallel updating on the microscopic time scale of AMM.

The type labels in Figure 3.1 of the form $\sigma_i$ characterise the configuration as follows: $\sigma = \alpha$ indicates that the active site carries three particles, $\sigma = \beta$ indicates that it carries two. The index $i$ indicates the number of neighbouring sites carrying a single particle post-toppling. In general, $i \in \{0, \ldots, q\}$

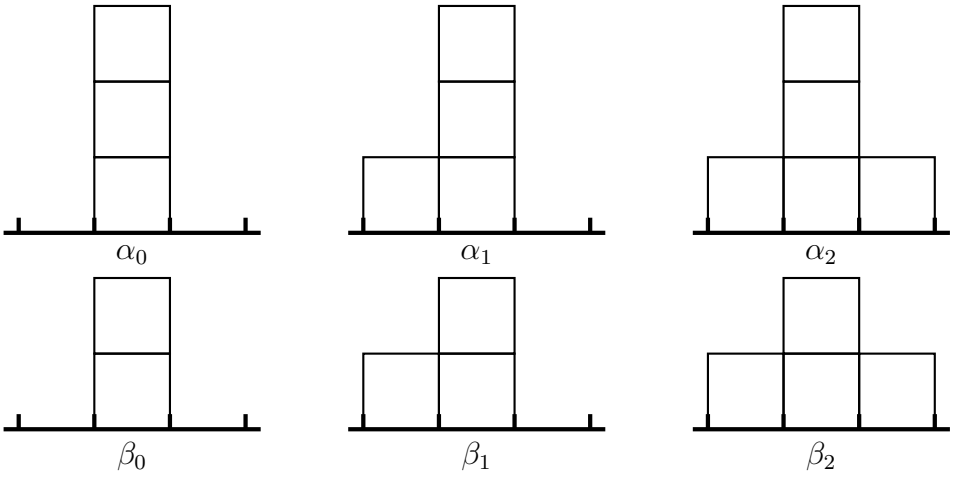



**Figure 3.1:** The six different *active motives* of the one-dimensional Abelian Manna model. The central site carries either three ($\alpha_i$ for $i = 0, 1, 2$) or two particles ($\beta_i$ for $i = 0, 1, 2$) and is to topple in the next microscopic time step. The occupation number of sites neighbouring the central site are representative only in as far as their parity is concerned, with $i$ indicating the number of sites that carry an odd number. Their occupation number is *post-toppling* (after *they* may have toppled themselves, but prior to the central site toppling), whereas the central site is shown *pre-topping* (before it topples). The configurations differ in whether neighbouring sites may or may not topple themselves due to being charged by the toppling site. Although we may picture the configurations being situated on a one-dimensional lattice, their spatial orientation is irrelevant and so we do not distinguish left and right neighbours.

where $q$ is the coordination number. Henceforth, we restrict ourselves to regular lattices with constant coordination number $q$. These may be thought of as $d$-dimensional hypercubic lattices with $q = 2d$.

At any point during the evolution of an avalanche, those sites whose occupation information is not captured by the active motives are occupied independently with density $\zeta$. The active sites we consider carry only ever two or three particles, *i.e.* we do not keep track of multiple topplings. In Figure 3.2 we illustrate how the toppling of motive $\alpha_1$ in one dimension gives rise to the motive $\beta_2$.

In the interest of clarity, we summarise our key assumptions: *(i)* In each timestep during an avalanche, the substrate sites (sites whose occupation information is not captured in the active motives) are assumed to be occupied

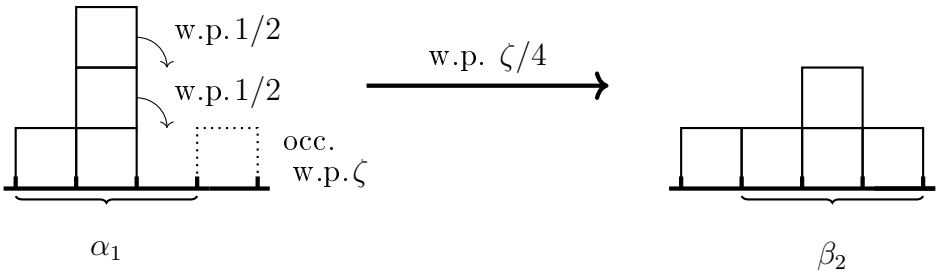



**Figure 3.2:** Example of a toppling on a one-dimensional lattice. The initial state $\alpha_1$ goes over into state $\beta_2$ with probability (w.p.) $\zeta/4$, which is the joint probability of three independent events: The independent toppling of two particles to one side (w.p. $1/4$) and the occupation of a next-nearest neighbouring site (w.p. $\zeta$). The latter assumption ignores spatial correlations.

independently with probability $\zeta$, which is a fixed model parameter. This is where we ignore correlations. *(ii)* No occupation number post-toppling exceeds unity and no active site carries more than three particles. This is a significant restriction only in one dimension, where multiple toppling is known to play a significant role [88]. *(iii)* No site receives particles toppling from different sites simultaneously. *(iv)* All sites are considered bulk sites, *i.e.* there is no boundary. Each site has therefore the same number $q$ of neighbours.

The time in the branching process progresses by all individuals attempting branching in each parallel timestep, which corresponds to the microscopic time in AMM. The branching itself mimics the toppling dynamics: In each toppling two particles are redistributed to the same neighbour with probability (w.p.) $1/q$ and to different neighbours w.p. $1-1/q$. For a configuration of type $\sigma_j$, a randomly chosen neighbour of the active, toppling site is occupied (has odd parity) w.p. $j/q$. The active site itself will be left occupied if $\sigma = \alpha$ and empty if $\sigma = \beta$. The next nearest neighbours of any active site are treated as substrate sites, occupied w.p. $\zeta$ and empty w.p. $(1-\zeta)$. An illustrative example of a branching path on a one-dimensional lattice is shown in Figure 3.2, where the motive $\alpha_1$ is shown to turn into $\beta_2$ w.p. $\zeta/4$. The probabilities of all branching paths on regular lattices with constant $q$ are listed in Tab. 3.1. The multi-type branching process initiates from a single

| parent | branching probability | offspring |
|---|---|---|
| $\alpha_j$ | $\frac{j}{q^2}$ $\mathrm{Bin}(k, q-1; \zeta)$ | $\alpha_{k+1}$ |
| | $\frac{(2j+1)(q-j)}{q^2}$ $\mathrm{Bin}(k, q-1; \zeta)$ | $\beta_{k+1}$ |
| | $\frac{j(j-1)}{q^2}$ $\mathrm{Bin}(k, q-1; \zeta)$ | $2\beta_{k+1}$ |
| | $\frac{(q-j)(q-j-1)}{q^2}$ $\mathrm{Bin}(k, q-1; \zeta)$ | $\varnothing$ |
| $\beta_j$ | $\frac{j}{q^2}$ $\mathrm{Bin}(k, q-1; \zeta)$ | $\alpha_k$ |
| | $\frac{(2j+1)(q-j)}{q^2}$ $\mathrm{Bin}(k, q-1; \zeta)$ | $\beta_k$ |
| | $\frac{j(j-1)}{q^2}$ $\mathrm{Bin}(k, q-1; \zeta)$ | $2\beta_k$ |
| | $\frac{(q-j)(q-j-1)}{q^2}$ $\mathrm{Bin}(k, q-1; \zeta)$ | $\varnothing$ |

**Table 3.1:** Branching probabilities of active motives on a regular lattice with constant coordination number $q$. The only form of branching occurs is when two independent copies of $\beta_k$ are generated, indicated by $2\beta_k$. The symbol $\varnothing$ indicates that no offspring is produced.

motif centred on the site that triggers the avalanche. Assuming uncorrelated occupation of sites in quiescent states at criticality, the initial motif is of type $\beta_j$ with probability

$$\mathrm{Bin}(j, q; \zeta) = \binom{q}{j} \zeta^j (1-\zeta)^{q-j}, \tag{3.1}$$

To keep the expressions below consistent, we allow $\mathrm{Bin}(j, q; \zeta) = 0$ for $j > q$.

The multi-type branching process defined above approximates the population dynamics of the activity in an avalanche of AMM on an infinite lattice. Activity performs a (branching) random walk on the lattice, as active sites topple and produce active offspring sites [89]. For avalanches on finite lattices with open boundaries, when the density is subcritical, the activity is expected to extinguish before particles reach any of the boundaries, and as a result, the occupation density $\zeta$ increases under the external drive. When supercritical, the activity with large probability persists until incurring dissipation at the boundaries which decreases the density accordingly [88]. On the other hand, large $\zeta$ will generally lead to larger avalanches, and small

$\zeta$ to small avalanches. Nevertheless, under this apparent self-organisation [30, 90], the fluctuations of $\zeta$ decrease with system size and in the thermodynamic limit, the stationary density approaches a particular value generally referred to as the critical density (even when there may be more than one, [91]). We identify the critical density as the smallest density $\zeta_c$ at which the multi-type branching process has a finite probability to evolve forever, *i.e.* its critical point, when the branching ratio is unity.

To find the critical point of the multi-type branching process, it suffices to determine the density $\zeta_c$ when the largest eigenvalue $\lambda_1$ of the mean offspring matrix $\mathbf{M}$ introduced below is unity [23, p186].

The mean offspring matrix is the matrix $\mathbf{M} = \{m_{\sigma,\tau}\}$, with $m_{\sigma,\tau}$ the mean number of offspring of type $\tau$ produced as an individual of type $\sigma$ undergoes multi-type branching, *i.e.* an update. The types $\sigma$ and $\tau$ are any of the states $\alpha_j$ and $\beta_j$ with $j \in \{0, 1, \ldots, q\}$, as exemplified in Figure 3.1. The individual elements $m_{\sigma,\tau}$ of the matrix are easily determined from Tab. 3.1,

$$m_{\alpha_j,\alpha_0} = 0 \tag{3.2a}$$

$$m_{\alpha_j,\alpha_k} = \frac{j}{q^2}\,\mathrm{Bin}(k-1, q-1; \zeta) \text{ for } k > 0 \tag{3.2b}$$

$$m_{\alpha_j,\beta_0} = 0 \tag{3.2c}$$

$$m_{\alpha_j,\beta_k} = \frac{(2j+1)q - 3j}{q^2}\,\mathrm{Bin}(k-1, q-1; \zeta) \text{ for } k > 0 \tag{3.2d}$$

$$m_{\beta_j,\alpha_k} = \frac{j}{q^2}\,\mathrm{Bin}(k, q-1; \zeta) \tag{3.2e}$$

$$m_{\beta_j,\beta_k} = \frac{(2j+1)q - 3j}{q^2}\,\mathrm{Bin}(k, q-1; \zeta). \tag{3.2f}$$

Because $m_{\alpha_j,\alpha_{k+1}} = m_{\beta_j,\alpha_k}$ and $m_{\alpha_j,\beta_{k+1}} = m_{\beta_j,\beta_k}$, the matrix $\mathbf{M}$ has some very convenient symmetries, which, after ordering states according to

$(\alpha_0, \ldots, \alpha_q, \beta_0, \ldots, \beta_q)$ may be written as

$$\mathbf{M} = \left( \begin{array}{c|c} \underline{0}_{q+1}, \underline{a} \bigotimes \underline{B} & \underline{0}_{q+1}, \underline{b} \bigotimes \underline{B} \\ \hline \underline{a} \bigotimes \underline{B}, \underline{0}_{n+1} & \underline{b} \bigotimes \underline{B}, \underline{0}_{q+1} \end{array} \right) \tag{3.3}$$

with vectors

$$\underline{a} = (a_j)_{0 \leqslant j \leqslant q} \quad \text{with} \quad a_j = j/q^2 \tag{3.4}$$

$$\underline{b} = (b_j)_{0 \leqslant j \leqslant q} \quad \text{with} \quad b_j = (2j+1)/q - 3j/q^2 \tag{3.5}$$

$$\underline{B} = (B_k)_{0 \leqslant k \leqslant q-1} \quad \text{with} \quad B_k = \mathrm{Bin}(k, q-1; \zeta) \tag{3.6}$$

and $\underline{0}_{q+1}$ is a column of $q+1$ zeroes. For example, the matrix for the one-dimensional AMM is

$$\mathbf{M} = \begin{pmatrix} 0 & 0 & 0 & 0 & \frac{1}{2}B_0 & \frac{1}{2}B_1 \\ 0 & \frac{1}{4}B_0 & \frac{1}{4}B_1 & 0 & \frac{3}{4}B_0 & \frac{3}{4}B_1 \\ 0 & \frac{1}{2}B_0 & \frac{1}{2}B_1 & 0 & B_0 & B_1 \\ 0 & 0 & 0 & \frac{1}{2}B_0 & \frac{1}{2}B_1 & 0 \\ \frac{1}{4}B_0 & \frac{1}{4}B_1 & 0 & \frac{3}{4}B_0 & \frac{3}{4}B_1 & 0 \\ \frac{1}{2}B_0 & \frac{1}{2}B_1 & 0 & B_0 & B_1 & 0 \end{pmatrix}, \tag{3.7}$$

using $B_0 = \mathrm{Bin}(0, 1; \zeta) = 1 - \zeta$, $B_1 = \mathrm{Bin}(1, 1; \zeta) = \zeta$ and $B_2 = \mathrm{Bin}(2, 1; \zeta) = 0$.

Upon factorisation, the characteristic polynomial of $\mathbf{M}$ obtains a surprisingly simple form:

$$\begin{aligned} &\det\big(\lambda \mathbf{I} - \mathbf{M}\big) = \\ &\lambda^{2q-2}\Big(\lambda^2 - \frac{1}{q^3}\Big)\Big[\lambda^2 - \frac{2(q-1)^2\zeta + q + 1}{q^2} + \frac{1}{q^3}\Big]. \end{aligned} \tag{3.8}$$

Since $q = 2d \geqslant 2$, the largest root $\lambda_1$ equals unity if and only if $\zeta = \frac{q+1}{2q}$. It exceeds unity if and only if $\zeta$ exceeds $\frac{q+1}{2q}$. Our estimate of the critical

| dimension | 1 | 2 | 3 | 5 |
|---|---|---|---|---|
| $\zeta_c$ (numerics) | 0.94882(1) [74] | 0.7170(4)[81] | 0.622325(1) [82] | 0.559780(5) [74] |
| $\zeta_c$ (present work) | 0.750 | 0.625 | 0.583 | 0.550 |

**Table 3.2:** The theoretical estimate of the critical density $\zeta_c$ in the $d$-dimensional AMM derived here compared to the numerical values reported in the literature for the stationary density of the Abelian Manna model.

density is thus

$$\zeta_c = \frac{q+1}{2q}. \tag{3.9}$$

This is the central result of the present work. Writing this result in a more suggestive form, with $q = 2d$ for hypercubic lattices we obtain $\zeta_c = \frac{1}{2} + \frac{1}{4d}$, *i.e.*, a correction to the mean-field result $\zeta_{c,(\mathrm{MF})} = \frac{1}{2}$ by $\frac{1}{4d}$. Tab. 3.2 shows a comparison between this result and the numerical values found by simulations [74, 81, 82] on lattices in dimensions $d \in \{1, 2, 3, 5\}$. While our estimate Eq. (3.9) underestimates $\zeta_c$ as found numerically by about 21% in one dimension, this deviation drops to about 2% in five dimensions. We would expect that incorporating a larger number of nearest neighbours would improve the estimate further [71].

### 3.2.1 The fixed-energy AMM on random regular graphs

In the derivation above the dimension $d$ of the hypercubic lattices considered enters only in as far as the coordination number $q = 2d$ is concerned. Hence the results equally apply to AMM on any graph with fixed coordination number. To demonstrate this, we compare numerical estimates of the critical density in random 5-regular graphs [92] ($q = 5$) to our theoretical approximation. To avoid the complication of choosing sinks or dissipation sites on graphs, we adopt the fixed-energy version of AMM [93] in the simulations. For a given density, particles are initially uniformly randomly distributed on the sites of the graph, and a random occupied site is driven to start the avalanche. To determine the critical density, we estimate the survival probability of the activity after many microscopic timesteps (approximately ten

times the size of the graph) and plot it against the particle density for different graph sizes $N$, Figure 3.3. The numerical estimate of $\zeta_c \approx 0.62$ as the apparent onset of a finite probability of indefinite survival is consistent with our theoretical approximate $\zeta_c = \frac{1}{2} + \frac{1}{2q} = 0.6$.

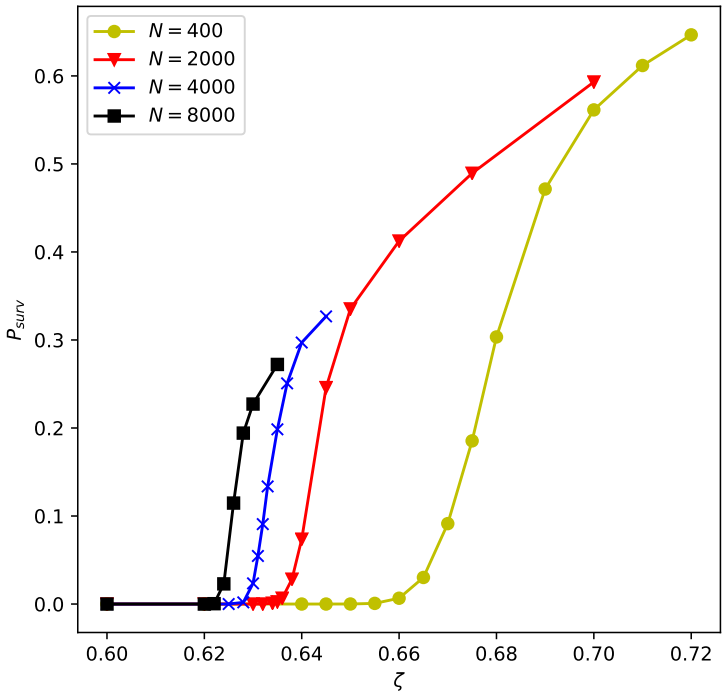



**Figure 3.3:** Estimate of the asymptotic density in the fixed-energy version of AMM on random 5-regular graphs of different sizes. The approximate critical point, identified as the onset of asymptotic survival, at around $\zeta_c = 0.62$ is very close to the theoretical prediction $\zeta_c = \frac{1}{2} + \frac{1}{2q} = 0.6$.

## 3.3 Summary and Discussion

In the procedure outlined above, we have cast the dynamics of the Abelian Manna model in a multi-type branching process, whose types consist of active motives of composite sites. Upon charging a singly occupied site a branching process ensues and evolves by producing offspring according to the density of occupied sites $\zeta$. The critical density $\zeta_c$ of the AMM is identified as the value of $\zeta$ when the branching process is critical, which we derived in a simple closed form, systematically improving on the mean-field prediction. Our main results Eq. (3.9) are in line with numerical findings in the literatures, Tab. 3.2. The most significant corrections are found in low dimensions and the estimates are with excellent accuracy in moderately high dimensions, e.g., $d = 5$.

It was recently established that the occupation numbers of AMM in the quiescent state display long-ranged anti-correlations [94, 95]. These correlations are *not* captured in the procedure outlined above. The corrections to the mean-field value that we find are solely based on the correlations of site-occupations that develop during the course of an avalanche.

The motives that we use to capture local occupancy and its correlations represent the occupancy of nearest neighbours only in as far as their parity after having (possibly) toppled themselves is concerned. The small number of motives allows us to find a closed form the critical density in arbitrary dimension and on more complicated graphs, in contrast to other well-known techniques such as cluster approximation [96, 71].

The method we introduced here also provide insights into the evolution of activity in AMM avalanches. AMM is believed to belong to the conserved directed percolation (CDP) universality class [93, 77], which is different from the more general directed percolation (DP) universality class due to the conservation of particles in the dynamics. In the present work, through the mapping of AMM avalanches to a MTBP, we explicitly show that the cor-

relation and conservation of particles during avalanching causes the shift of the critical density away from its mean-field value. During an avalanche, activity grows (active motives split) at the cost of singly-occupied sites, so that the sites receiving toppling particles are occupied with a probability less than their mean density. The conservation of particles and their spatial correlation thus lead to local suppression of activity. The MTBP mapping respects particle conservation within active motives, which keep track only of the total number of particles post-toppling at the neighbours of an active site. Our method does not keep track of the total number of particles in the system, but numerical evidence strongly suggests that this fluctuates very little in large systems [74], indicating that activity is much less affected by global conservation.

It would be interesting for future work to establish a rigorous lower bound of $\zeta_c$ by considering the activity of AMM as some critical population dynamics, e.g. via the coupling method [97].

# 4

# Field-Theoretic Approach to Reacting Particle Systems

This chapter is partially based on the paper [98] "*Volume explored by a branching random walk on general graphs*", Scientific reports 9, no. 1 (2019): 1-9, by Ignacio Bordeu, Saoirse Amarteifio, Rosalba Garcia-Millan, Benjamin Walter, Nanxin Wei, and Gunnar Pruessner.
The paper is the result of a group project led by GP, which NW participated in. The main contribution of NW to [98] is discussed in **section 4.3**. The Feynman diagrams used in this chapter are adapted from the manuscript of [98], originally produced by IB and GP.

To go beyond (effective) mean-field theories for interacting particle systems, we have to take into account long-range spatio-temporal correlations.

One systematic way of treating such correlations is through field-theoretic methods. There are many formulations of (statistical) field theories [99, 15]. Here we limit our attention to the so-called Doi-Peliti formalism [100, 101] for reacting particle systems, which constructs field theories from microscopic dynamics in a faithful representation before taking the continuum limit, thus bearing the advantage of capturing discrete stochasticity of particles. We first give a brief introduction to the Doi-Peliti formalism of field theories and what can be calculated from there, then showcase this approach in two examples and report on some of the results from field-theoretic analysis. Finally, we try to generalise the field-theoretic methods to reacting diffusive particle systems on networks.

## 4.1 Brief Introduction to the Doi-Peliti Formalism of Field Theories

Consider particle systems on discrete structures, typically $d$-dimensional hypercubic lattices ($d = 0$ corresponds to a single site). Denote particle types as $A$, $B$, ..., then a particle configuration is given by $\{n_{\text{A}}(\mathbf{x})n_{\text{B}}(\mathbf{x})\cdots\}$ where $\mathbf{x}$ represents coordinates of sites. Particles are subject to a set of dynamical rules of *on-site reactions* and *hopping*, both Markovian, see e.g. [102, 5]. The dynamics of the system is thus described by a set of master equations governing the evolution of the probability distribution of particle configurations $P(n_{\text{A}}(\mathbf{x})n_{\text{B}}(\mathbf{x})\cdots, t)$, much like Eq.(1.2.1).

The first step of the Doi-Peliti formalism is to encode particle configurations in a Fock space representation of bosonic particles as $|n_{\text{A}}(\mathbf{x})n_{\text{B}}(\mathbf{x})\cdots\rangle$, and their probability distribution at time $t$ as

$$|\Psi(t)\rangle := \sum_{\{n_{\text{A}}(\mathbf{x})n_{\text{B}}(\mathbf{x})\cdots\}} P(n_{\text{A}}(\mathbf{x})n_{\text{B}}(\mathbf{x})\cdots, t)\,|n_{\text{A}}(\mathbf{x})n_{\text{B}}(\mathbf{x})\cdots\rangle \tag{4.1.1}$$

Each type of particle is equipped with a set of *creation* and *annihilation* operators, e.g., type $A$ with $a^\dagger(\mathbf{x})$ and $a(\mathbf{x})$, which act on configurations as

$$\begin{aligned} a^\dagger(\mathbf{x})\,|n_{\text{A}}(\mathbf{x})n_{\text{B}}(\mathbf{x})\cdots\rangle &= |n_{\text{A}}(\mathbf{x})+1, n_{\text{B}}(\mathbf{x})\cdots\rangle \\ a(\mathbf{x})\,|n_{\text{A}}(\mathbf{x})n_{\text{B}}(\mathbf{x})\cdots\rangle &= n_{\text{A}}(\mathbf{x})\,|n_{\text{A}}(\mathbf{x})-1, n_{\text{B}}(\mathbf{x})\cdots\rangle \end{aligned} \tag{4.1.2}$$

The master equations can then be presented compactly in an operator form

$$\frac{d}{dt}\,|\Psi(t)\rangle = -\hat{H}\,|\Psi(t)\rangle\,, \tag{4.1.3}$$

with the stochastic pseudo-Hamiltonian $\hat{H} = \hat{H}(a^\dagger(\mathbf{x}), a(\mathbf{x}), b^\dagger(\mathbf{x}), b(\mathbf{x}), \cdots)$ encoding the full dynamics of the system. The solution of Eq.(4.1.3) can be formally written as

$$|\Psi(t)\rangle = e^{-\hat{H}t}\,|\Psi(0)\rangle \tag{4.1.4}$$

Observables of interest are measured as average over $P(n_{\text{A}}(\mathbf{x})n_{\text{B}}(\mathbf{x})\cdots, t)$ (or distributions of multiple times), which can be extracted from the state of the system $|\Psi(t)\rangle$, e.g.,

$$\langle\hat{\mathcal{O}}\rangle = \langle\text{☼}|\,\hat{\mathcal{O}}\,|\Psi(t)\rangle = \langle\text{☼}|\,\hat{\mathcal{O}}e^{-\hat{H}t}\,|\Psi(0)\rangle\,, \tag{4.1.5}$$

where the observable $\hat{\mathcal{O}} = \hat{\mathcal{O}}(a^\dagger(\mathbf{x}), a(\mathbf{x}), b^\dagger(\mathbf{x}), b(\mathbf{x}), \cdots)$ and the projection operator $\langle\text{☼}| = \langle 0|\exp\{a(\mathbf{x})b(\mathbf{x})\cdots\}$.

Following the standard procedure [103, 104] of discretising the time interval and inserting complete sets of coherent states, we can transform Eq.(4.1.5) into a path integral given as

$$\langle\mathcal{O}\rangle = \int \mathcal{D}[\phi_1^\dagger, \phi_1, \phi_2^\dagger, \phi_2, \cdots]\mathcal{O}e^{\mathcal{A}[\phi_1^\dagger,\phi_1,\phi_2^\dagger,\phi_2,\cdots]}, \tag{4.1.6}$$

where $\mathcal{O} = \mathcal{O}(\phi_1^\dagger, \phi_1, \phi_2^\dagger, \phi_2, \cdots)$ is obtained from replacing operators $a^\dagger(\mathbf{x}), a(\mathbf{x})$ with fields $\phi_1^\dagger(\mathbf{x}), \phi_1(\mathbf{x})$ and $b^\dagger(\mathbf{x}), b(\mathbf{x})$ with fields $\phi_2^\dagger(\mathbf{x}), \phi_2(\mathbf{x})$, etc., and the *action* $\mathcal{A} = -\int d\mathbf{x}dt\mathcal{L}$ from the space-time integral of the *Liouvillian* $\mathcal{L}$ adapted from replacing operators with corresponding fields in $\hat{H}$. To sim-

plify the field-theoretic action $\mathcal{A}$, we apply the so-called *Doi-shift* by changing the variables for creation fields $\widetilde{\phi} = \phi^\dagger - 1$.[1]

$\mathcal{L}(\widetilde{\phi}_1, \phi_1, \widetilde{\phi}_2, \phi_2, \cdots)$ consists of a bilinear Gaussian part which represents *free fields*, and the rest representing *interactions*. For the perturbative methods of field theory (to which we limit our discussions), observables are evaluated from the path integral as perturbation expansion, i.e., the sum of a series of correlation functions (most conveniently in the moment space) evaluated under the Gaussian measure of free fields. The expansion series can be neatly expressed in *Feynman diagrams* [105], composed of bare *propagators* with associated *masses* (free fields) and *vertices* with bare *couplings* (interactions). Note that in the Doi-Peliti formalism, after the Doi-shift, diagrams do not directly corresponds to particle reactions, but correlations generated from reactions.

Presented in diagrammatics, perturbation expansion can be seen as loop expansion, with tree diagrams as the 0-th order. From the physical interpretation of diagrams mentioned above, it is clear that tree diagrams account for contributions to an observable neglecting dynamical correlations (which involve the spatial-temporal history of participating particles). As such, keeping only tree diagrams corresponds to a mean-field theory (approximation).[2] Contributions of loop diagrams can be summed up as *Dyson sum* featuring *one-particle irreducible diagrams* or *proper vertices* [105]. The number of loops in a proper vertex determines its order in the loop expansion, thus one can include contributions to an observable up to one-loop diagrams, two-loop diagrams, etc, as corrections to the tree-level / mean-field calculation, by considering only possible proper vertices up to that order.

Formally, loop diagrams are integrals over the entire momentum space and involve singularities, being that *infrared* (IR), *ultraviolet* (UV) or *logarithmic*

[1] The procedure described here can be better understood through the examples in the next section.

[2] We shall see that BP has only tree diagrams and are indeed exact mean-field theories.

divergence depending on the dimension of the field theory. In our current context, i.e., particle systems defined on lattices (or other discrete structures), if the contributing loop diagram is UV-divergent, then it can be naturally *regularised* (made finite) by imposing an upper cut-off in the momentum space due to the minimum spacing of the lattice. Notably, contributions from such loop diagrams amount to a *finite* correction to observables and do *not* change the related critical behaviours.

On the other hand, if the contributing loop diagram poses IR- or logarithmic divergence, the loop expansion hence the perturbation expansion can not be understood as summing up the bare values of terms included. However, if we are interested in critical behaviours, thanks to the ansatz of scale-invariance at criticality, the loop expansion may yet be interpreted as a relation of (IR- or log-) scaling limits. To systematically extract scaling limits of correlation functions with divergent loop contributions, one resort to (moment space) *renormalisation group* (RG) methods [99, 15]. There are a number of recipes for RG, all involve the transformations of fields and couplings induced by probing the system at varying momentum scales. Going down with momentum scales, such transformations form a RG flow, leading to stable fixed point(s) featuring scale-invariant critical behaviours. The renormalised couplings at each stable fixed point of the RG flow thus characterise a *universality class*.

To ensure renormalisability, one extra step is required before the RG analysis. Note that loop diagrams are constructed by propagators and interaction vertices. Given the spatial dimension $d$ of the field theory, from dimensional analysis (power counting), we can deduce the *momentum scaling dimension* of each coupling of interaction vertices: positive, zero or negative corresponding to the coupling being *relevant*, *marginal* or *irrelevant* respectively. Here, "relevant" means that the coupling is relevant for constructing IR-divergent loop diagrams, and "marginal" and "irrelevant" in the same vein. The *upper critical dimension* $d_c$ is identified as the dimension that keeps a minimum set of couplings marginal and renders the rest irrelevant. As such, when the

field theory is in dimension $d > d_c$, all of the interactions are irrelevant for IR-singularity, hence we expect mean-field critical behaviours following from the Gaussian (trivial) fixed point of the RG flows.
When $d \leqslant d_c$, the field theory admits corrections from IR- or logarithmically divergent loop diagrams and the RG flows may lead to non-trivial stable fixed point(s) signifying alternative critical behaviours.

We have briefly cruised through the construction of field theories via Doi-Peliti formalism and the pipeline of field-theoretic analysis, with much technical details omitted. The purpose of such account is only to introduce the necessary concepts and key ingredients that enable the understanding of results we report in the next section and the discussion in the section to follow.

## 4.2 Examples of Field Theories *à la* Doi-Peliti

### 4.2.1 Field theory of activated random walk

We need two types of particles to describe the exact AMM avalanche process: the active particles labelled $A$ and the substrate particles labelled $B$.

$$A + B \xrightarrow{u} 2A \qquad a^{\dagger 2}ba - conjug. \tag{4.2.1}$$

$$A \xrightarrow[(n_B=0)]{u} B \qquad b^\dagger(1 - b^\dagger b)a - conjug. \tag{4.2.2}$$

In addition, active particles $A$ hop or random walk to nearest neighbouring sites with effective diffusivity $D$, while substrate particles $B$ stay immobile.

$$a^{\dagger 2}ba - b^\dagger b a^\dagger a = (\tilde{a}^2 + \tilde{a})ba - \tilde{b}(\tilde{a} + 1)ba \tag{4.2.1'}$$




(4.2.1a)

(4.2.1b)

$$b^\dagger(1-b^\dagger b)a-(1-b^\dagger b)a^\dagger a=(\tilde{b}-\tilde{a})a+\tilde{a}(\tilde{b}+1)ba-(\tilde{b}^2+\tilde{b})ba \tag{4.2.2'}$$




(4.2.2a)

(4.2.2b)

(4.2.2c)

$$-H=-D\nabla\widetilde{\phi}\nabla\phi+u(\widetilde{\phi}-\widetilde{\psi})\phi+2u(\widetilde{\phi}-\widetilde{\psi})\psi\phi+u(\widetilde{\phi}^2-\widetilde{\psi}^2)\psi\phi \tag{4.2.3}$$

$$\begin{aligned}-\mathcal{L}=&-\widetilde{\phi}\partial_t\phi-\widetilde{\psi}\partial_t\psi-\epsilon_b\widetilde{\psi}\psi+D\widetilde{\phi}\nabla^2\phi\\&+u(\widetilde{\phi}-\widetilde{\psi})\phi+2u(\widetilde{\phi}-\widetilde{\psi})\psi\phi+u(\widetilde{\phi}^2-\widetilde{\psi}^2)\psi\phi\end{aligned} \tag{4.2.4}$$

### 4.2.2 Field theory of branching Wiener sausages

"Branching Wiener sausages" refer to distinct sites visited by branching random walkers, generalising from "Wiener sausage" as distinct sites visited by random walkers in the continuum limit.

$$A \xrightarrow{rp_k} kA, \qquad k = 0, 2 \qquad\qquad a^{\dagger k}a - conjug. \qquad (4.2.5)$$

$$A \xrightarrow[(n_B=0)]{u} A + B \qquad\qquad b^\dagger(1 - b^\dagger b)a^\dagger a - conjug. \qquad (4.2.6)$$

In addition, active particles $A$ hop or random walk to nearest neighbouring sites with effective diffusivity $D$, while ink particles $B$ stay immobile.

$$r[p_0(a - a^\dagger a) + p_2(a^{\dagger 2}a - a^\dagger a)] = -r(1 - 2p_2)\tilde{a}a + rp_2\tilde{a}^2 a \qquad (4.2.5')$$




(4.2.5a)

$$b^\dagger(1 - b^\dagger b)a^\dagger a - (1 - b^\dagger b)a^\dagger a = \tilde{b}(\tilde{a} + 1)a - (\tilde{b}^2 + \tilde{b})(\tilde{a} + 1)ba \qquad (4.2.6')$$

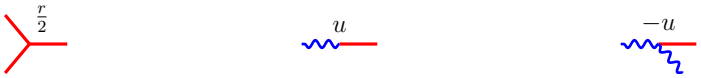



(4.2.6a)

(4.2.6b)

(4.2.6c)

Dimensional analysis give the critical dimension $d_c = 4$, the only relevant interaction couplings are (4.2.5a)-right, (4.2.6a)-left and (4.2.6b)-left:

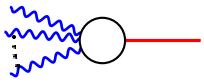


$$-\mathcal{L} \doteq -\widetilde{\phi}\partial_t\phi - \widetilde{\psi}\partial_t\psi - \epsilon_a\widetilde{\phi}\phi - \epsilon_b\widetilde{\psi}\psi + D\widetilde{\phi}\nabla^2\phi + \frac{r}{2}\widetilde{\phi}^2\phi + u\widetilde{\psi}\phi - u\widetilde{\psi}\psi\phi \tag{4.2.7}$$

The observables interested, moments of the distinct site visited is given by

$$\langle N_b^n \rangle = \int \mathrm{d}^d x_n \cdots \mathrm{d}^d x_1 \langle \psi(\mathbf{x}_n, t) \cdots \psi(\mathbf{x}_1, t)\widetilde{\phi}(\mathbf{x}_0, 0)\rangle \tag{4.2.8}$$

diagrammatic as

 (4.2.9)

The critical dimension $d_c = 4$.
The scaling of the $n$-th moment of the number of distinct sites visited
If $d < 2$ this volume remains finite in large $t$.

If $2 \leqslant d < 4$ (provided that $nd - 2 > 0$)

$$\langle N_b^n \rangle (t, l) \sim \begin{cases} t^{(nd-2)/2} & Dt \ll l^2 \\ l^{nd-2} & Dt \gg l^2 \end{cases} \tag{4.2.10}$$

If $d \geqslant 4$

$$\langle N_b^n \rangle (t, l) \sim \begin{cases} t^{2n-1} & Dt \ll l^2 \\ l^{4n-2} & Dt \gg l^2 \end{cases} \tag{4.2.11}$$

## 4.3 Critical Dynamics of Reacting Diffusive Particle Systems on Networks

Hitherto we have discussed field-theoretic methods for reacting diffusive particle systems defined on a hypercubic lattice and its continuum limit, the $d$-dimensional Euclidean space. It is then natural to try to generalise

these powerful methods to particle systems on inhomogeneous structures, especially tempting for the vibrant area of network dynamics.

Consider the particle system of branching random walkers described in **subsection 4.2.2**, now on a undirected network $G$ with $N$ nodes. The dynamics only differ from the lattice version in terms of hopping of active particles as random walkers. Assume active particles perform continuous-time, unbiased *edge-based* (or edge-centric) random walks [106] with unit rate on $G$ in addition to on-node reactions (branching and deposition), i.e., each active particle on a node hops to one of its nearest neighbours *each* with unit rate. At the master equation level, this corresponds to taking the (unnormalised) *graph Laplacian* $\mathbf{L} := \mathbf{D} - \mathbf{A}$ as the diffusion operator. Here $\mathbf{D} := \mathrm{diag}(d_1, \ldots, d_N)$ is the diagonal matrix with node degrees as entries and $\mathbf{A}$ the adjacency matrix. The field theory of this system can be obtained simply by replacing the Euclidean diffusion operator $-D\nabla^2$ with $\frac{1}{2}\mathbf{L}$ in the Liouvillian, fields in spatial coordinates with vector fields, and summing over all node indices instead of integrating over space in the field-theoretic action $\mathcal{A}$. To focus on critical dynamics, again we keep only relevant interactions and the new action reads

$$\begin{aligned}\mathcal{A} \doteq \int \mathrm{d}t \big[ & -\widetilde{\boldsymbol{\phi}}^{\mathrm{T}} \partial_t \boldsymbol{\phi} - \widetilde{\boldsymbol{\psi}}^{\mathrm{T}} \partial_t \boldsymbol{\psi} - \epsilon_a \widetilde{\boldsymbol{\phi}}^{\mathrm{T}} \boldsymbol{\phi} - \epsilon_b \widetilde{\boldsymbol{\psi}}^{\mathrm{T}} \boldsymbol{\psi} \\ & - \tfrac{1}{2} \widetilde{\boldsymbol{\phi}}^{\mathrm{T}} \mathbf{L} \boldsymbol{\phi} + \tfrac{r}{2} (\widetilde{\boldsymbol{\phi}}^{\mathrm{T}})^2 \boldsymbol{\phi} + u \widetilde{\boldsymbol{\psi}}^{\mathrm{T}} \boldsymbol{\phi} - u \widetilde{\boldsymbol{\psi}}^{\mathrm{T}} (\boldsymbol{\psi}\boldsymbol{\phi}) \big],\end{aligned} \tag{4.3.1}$$

where $\widetilde{\boldsymbol{\phi}}$, $\boldsymbol{\phi}$, $\widetilde{\boldsymbol{\psi}}$, $\boldsymbol{\psi}$ are $N$-dimensional column vectors, $()^{\mathrm{T}}$ for transpose, and $(\widetilde{\boldsymbol{\phi}}^{\mathrm{T}})^2$, $(\widetilde{\boldsymbol{\psi}}\boldsymbol{\phi})$ to be understood as Hadamard products (element-wise product).

Path integrals with respect to the new action can be expressed by the same set of Feynman diagrams for perturbation expansion. As diagrams are calculated in the momentum space for Euclidean field theories, i.e., the eigenspace of the diffusion operator with Fourier modes as eigenbasis, similar calculations should be done in the eigenspace of $\mathbf{L}$ for field theories on networks. The eigenvalues and eigenvectors of $\mathbf{L}$ bear some well-known useful properties [107, 108]:

*(i)* Since $\mathbf{L}$ is real and symmetric, its eigenvalues (*spectrum*) $\{\lambda_i\}$ are real and can be associated to a set of real, normalised orthogonal eigenbasis $\{\boldsymbol{\xi}_{\lambda_i}\}$.
*(ii)* The smallest eigenvalue is 0, with eigenvector $\mathbf{1}$, and non-degenerate if and only if $G$ is connected. Let $0=\lambda_0<\lambda_1\leqslant\cdots\leqslant\lambda_{\mathrm{N}-1}$.
*(iii)* $\lambda_{\mathrm{N}-1}\leqslant 2k_{\max}$, where $k_{\max}$ is the largest degree of $G$. We consider sparse networks, with finite $k_{\max}$ even in the thermodynamic limit $N\to\infty$.
Define the *density of states* and (normalised) *spectral density* as

$$\rho(\lambda):=\sum_{i=0}^{N-1}\delta(\lambda-\lambda_i) \tag{4.3.2}$$

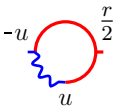
$$\rho_{\mathrm{n}}(\lambda):=\frac{1}{N}\rho(\lambda) \tag{4.3.3}$$

tree diagrams, mean-field critical behaviour as Eq.(4.2.11)

$$\langle N_b^n\rangle(t)\sim t^{2n-1},\qquad\qquad t\ll l^2(G) \tag{4.3.4}$$

where $l(G)$ stands for the diameter of $G$.

loop diagrams, consider only proper vertices, e.g.,

$\mathcal{U}_1=$ 

(4.3.5)

The lattice version reads

$$\begin{aligned}\mathcal{U}_1&=\int\mathrm{đ}\omega\mathrm{đ}^dq\,\frac{r/2}{-\mathring{\imath}\omega+Dq^2+\epsilon_a}\frac{u}{-\mathring{\imath}\omega+\epsilon_b}\frac{-u}{\mathring{\imath}\omega+Dq^2+\epsilon_a}\\&=\frac{-ru^2}{2}\int\mathrm{đ}\omega\mathrm{đ}^dq\left[(-\mathring{\imath}\omega+\epsilon_b)\big(\omega^2+(Dq^2+\epsilon_a)^2\big)\right]^{-1}\end{aligned} \tag{4.3.6}$$

where $\mathrm{đ}\omega=\mathrm{d}\omega/(2\pi),\mathrm{đ}^dq=\mathrm{d}^d\mathbf{q}/(2\pi)^d$ and $q^2=\mathbf{q}\cdot\mathbf{q}$, $\mathbf{q}$ being the momentum

and $\omega$ the frequency carried by the propagator. The network version reads

$$\begin{aligned}\mathcal{U}_1 =& \int \mathrm{đ}\omega \sum_{\lambda,\lambda'} \frac{r/2}{-\mathring{\imath}\omega + \lambda/2 + \epsilon_a} \frac{u}{-\mathring{\imath}\omega + \epsilon_b} \frac{-u}{\mathring{\imath}\omega + \lambda'/2 + \epsilon_a} \mathcal{V}_1(\lambda_0, \lambda, \lambda') \mathcal{V}_2(\lambda, \lambda') \\ =& \frac{-ru^2}{2} \int \mathrm{đ}\omega \, \mathrm{d}\lambda \rho(\lambda) \left[ (-\mathring{\imath}\omega + \epsilon_b) \left( \omega^2 + (\lambda/2 + \epsilon_a)^2 \right) \right]^{-1} \end{aligned} \tag{4.3.7}$$

where $\mathcal{V}_1(\lambda_0, \lambda, \lambda') = \sum_i \boldsymbol{\xi}_\lambda(i) \boldsymbol{\xi}_{\lambda'}(i) \boldsymbol{\xi}_0(i) = \delta_{\lambda,\lambda'}$ and $\mathcal{V}_2(\lambda, \lambda') = \sum_j \boldsymbol{\xi}^{\mathrm{T}}_\lambda(j) \boldsymbol{\xi}^{\mathrm{T}}_{\lambda'}(j) = \delta_{\lambda,\lambda'}$, due to the orthogonality of the eigenbasis and the fact that $\boldsymbol{\xi}_0 = \mathbf{1}$. Note that eigenvalue identities at vertices like the ones listed above in general do *not* hold for arbitrary field theory on networks, unlike the way they are guaranteed on lattices by the conservation of momentum as a result of translational invariance.

For many typical network ensembles, in the thermodynamic limit $N \to \infty$, the spectral density $\rho_{\mathrm{n}}$ converges to a continuous bulk distribution and sometimes accompanied by zero-measure (isolated) outliers [109, 110]. If 0 is an outlier, i.e., $\lambda_1 > 0$ in the thermodynamic limit, we say the Laplacian spectrum admits a *spectral gap*. necessarily mean-field, recover the scaling in Eq.(4.3.4)
If no spectral gap, $\lambda_1 \downarrow 0$ as $N \to \infty$. "infared" singularity in the loop integral
If further the infared end of the spectrum is governed by a spectral dimension $\tilde{d}$ such that

$$\rho_{\mathrm{n}}(\lambda) \sim \lambda^{\tilde{d}/2-1} \tag{4.3.8}$$

then the spectral dimension takes the place of the Euclidean dimension $d$ in characterising the critical behaviour. Thus if $\tilde{d} < \tilde{d}_c = 4$, then

$$\langle N_b^n \rangle (t) \sim t^{(n\tilde{d}-2)/2}, \qquad t \ll l^2(G) \tag{4.3.9}$$

The results are in good consistence with the numerical simulations, as shown in [98].

In conclusion, we hypothesise that for reacting particle systems on largely random networks, if the mobility is limited to edge-based random walks and

the reactions involve no more than three-leg vertices, then the results from field-theoretic analysis on the analogous lattice model can be translated over. If the networks admit a spectral gap, we expect mean-field critical behaviours; Otherwise we just replace the Euclidean dimension $d$ with the spectral dimension $\tilde{d}$ of the networks for critical scaling behaviours.

# 5

# Threshold Dynamics on Complex Networks and Message-Passing Methods

This chapter is partially based on the papers
"*Generalised Cascade Condition for Watts Threshold Model on Complex Networks*" by Nanxin Wei, Qing Yao and James P. Gleeson, in preparation;
and "*Persistent Threshold Dynamics with Recovery in Complex Networks*" by Nanxin Wei and Bo Fan, arXiv:1905.08358.
NW is the main contributor to both papers, in theory, simulations and manuscript writing.
QY produced Figure 5.2 and Figure 5.3, with some of NW's code.
The chapter contains **verbatim** reproduction from both manuscripts listed above without citation. Any other citations follow standard protocols.

In previous chapters, we've touched upon handling network dynamics as plain MFT (**Chapter 1**), effective MFT (**Chapter 3**) and methods to go beyond MFT (**Chapter 4**). In particular, **Chapter 3&4** show that mean-field approximation is highly successful for network dynamics and that it is quite challenging to go beyond MFT except for in special cases. In this chapter we introduce another theoretical method, message-passing, for network dynamics which directly take into account a most commonly used approximation for network topologies, i.e., locally tree-like assumption. We shall see that the message-passing method is closely related to MFT, yet not quite in some variants.

## 5.1 Watts Threshold Model and Abrupt Transitions

Threshold dynamics on complex networks has received a lot attention from researchers in recent years [18, 111]. In general, it refers to the spreading of a certain node state only enabled (or significantly facilitated) when a local threshold of collective vertex states is met. It also often appears in the literature under the name of complex or cooperative contagion [112, 113, 114, 115], in contrast to simple contagion dynamics such as the contact process where individual node state contribute to spreading independently. A consecutive of nodes meeting thresholds during the spreading process form a *cascade* [1], which are prevalent in the modelling of a variety of complex systems, e.g., the spreading of opinion [116] or adoption of innovation [117, 118] on social networks with peer pressure; the resilience of financial networks against default [119, 120], infrastructure networks against failure [121] or biological networks against ageing [122].

One important formulation of threshold dynamics is the Watts Threshold Model (WTM) proposed in [123], using a fractional threshold and allowing

[1] Synonymous to "avalanche", chosen here simply for consistency with existing literatures on this topic.

randomness in threshold determination. In some parameter regime of WTM, a small initial trigger may lead to a much larger cascade[2]. The condition for such *global cascades* is the focus of Watts' original work[123], and has since been systematically improved [124, 125, 126] and extensively studied in different variations [127, 128, 129, 130, 131].

On the other hand, WTM as cooperative spreading process is expected to exhibit an abrupt phase transition without the restriction of small trigger size. At the critical point of the transition, a small increase in trigger size would cause a jump in the final cascade size. In this sense, the global cascade condition mentioned above corresponds to the special case where the critical point is close to zero.

In this section, we study the condition of abrupt transitions for WTM in comparison with the classic global cascade condition via message-passing methods [124, 126, 132]. For random network ensembles, an extended phase diagram with three regions is obtained. The critical line marking the existence of a discontinuous (hybrid) transition is the generalised cascade condition. For fixed finite network, we take a dynamical perspective and derive an analogous condition of explosive cascading. A critical threshold criterion is proposed for arbitrary seed size, with the boundary case being the counterpart of the generalised cascade condition.

### 5.1.1 WTM on random networks

We first consider uncorrelated random network ensembles (configuration model [133]) with degree distribution $\{p_k\}$ in the thermodynamic limit (network size $N \to \infty$). Assume $\{p_k\}$ is unimodal and has finite mean $z := \langle k \rangle < \infty$, and that all relevant functions involving $\{p_k\}$ in this work is analytic (which can be ensured, e.g., by choosing sufficiently large maximum

[2]More precisely, a sublinear fraction $o(N)$ of nodes as trigger may lead to a cascade of linear fractional size $O(N)$ with high probability in the thermodynamic limit $N \to \infty$.

degree cut-off $k_{\max}$). The dynamics of WTM follows the standard set-up [123]:
$(i)$ Each node in the network can take one of the two states: *undamaged* or *damaged*.
$(ii)$ Each node is assigned a *fractional threshold*, say node $j$ is assigned $\hat{\theta}_j \in [0,1]$; $\hat{\theta}_j$ is drawn from a (cumulative) distribution $F_{\hat{\theta}}(\bullet)$ independent of $j$, typically parameterised with the mean threshold $\theta = \langle \hat{\theta} \rangle$.
$(iii)$ Initially a fraction $\mu$ (referred to as *trigger size*) of nodes are set as damaged, the rest undamaged.
$(iv)$ Damaged states spread through *threshold cascading*, updated in discrete time-steps denoted by $t$: If a node $j$ with degree $k_j$ and threshold $\hat{\theta}_j$ is undamaged and has $m$ damaged neighbours at time $t$ that satisfies $m/k_j > \hat{\theta}_j$ (the fraction of damaged neighbours exceeds its threshold), then node $j$ is damaged at time $t+1$.
$(v)$ Cascading continues until no threshold of the remaining undamaged nodes is exceeded. The average final fraction of damaged nodes[3], is referred to as the *final cascade size* $\rho$.

Given the network topology and threshold distribution, the final cascade size $\rho$ can be calculated from the trigger size $\mu$ via message-passing methods [126] under locally tree-like approximation. Let $\rho^{(t)}$ be the probability of an arbitrary node being damaged and average *message* $\nu^{(t)}$ the probability of one end of an arbitrary edge being damaged if the other end is *in cavity* (not contributing to damage spreading) at time $t$, we have:

$$\rho^{(t+1)} = \mu + (1-\mu) g(\nu^{(t)}) \qquad t = 0, 1, ... \tag{5.1.1}$$
$$g(x) = \sum_{k=1}^{\infty} p_k \sum_{m=0}^{k} \binom{k}{m} x^m (1-x)^{k-m} R(m,k)$$

[3] Technically to average over realisations of the network ensemble, threshold distribution and triggering sets of nodes; When assuming thermodynamic limit, equivalent to average over just realisations of triggering sets.

and

$$\nu^{(t+1)} = \mu + (1-\mu)h(\nu^{(t)}) \qquad t = 0, 1, ... \tag{5.1.2}$$
$$h(x) = \sum_{k=1}^{\infty} \frac{kp_k}{z} \sum_{m=0}^{k-1} \binom{k-1}{m} x^m (1-x)^{k-m-1} R(m,k)$$

where the response function for WTM $R(m,k)$ is the probability of a node with degree $k$ get damaged by a minimum of $m$ damaged neighbours given by

$$R(m,k) = \mathbb{P}\left\{\hat{\theta} < \frac{m}{k}\right\} = F_{\hat{\theta}}\left(\frac{m}{k}\right) \tag{5.1.3}$$

By definition $\rho^{(0)} = \nu^{(0)} = \mu$. Take the limit of iterations for Eq.(5.1.1) and Eq.(5.1.2), we have $\rho := \rho^{(\infty)}$ and $\nu := \nu^{(\infty)}$ satisfying:

$$\rho = \mu + (1-\mu)g(\nu) \tag{5.1.4}$$
$$\nu = \mu + (1-\mu)h(\nu) \tag{5.1.5}$$

Given $\mu$, Eq.(5.1.5) is a self-consistent equation about $\nu$. However, Eq.(5.1.5) may not have a unique solution. For the convenience of further analysis, we define $\Psi(x,\mu) := \mu + (1-\mu)h(x)$ and rewrites Eq.(5.1.2) as

$$\nu^{(t+1)} = \Psi(\nu^{(t)}, \mu) \qquad \mu \in [0,1) \tag{5.1.6}$$

$\nu$ is the iteration limit of Eq.(5.1.6), hence a fixed point of the mapping $\Psi(\bullet, \mu)$. Also, it should be a stable fixed point considering the randomness in triggering sets and the interpretation of $\nu$ as the average message. Since $\Psi(\bullet, \mu)$ is smooth and monotonically increasing, $\nu^{(0)} = \mu = \Psi(0,\mu) \geqslant 0$, $\Psi(1,\mu) \leqslant 1$, such stable fixed points exist in $[0,1]$ and $\nu$ is the smallest one of them.

When ($\mu=0\,\nu=0$) is a fixed point. The zero fixed point is unstable if and only if

$$\begin{aligned} & h'(0) > 1 \\ \Leftrightarrow \quad & \sum_{k=1}^{\infty} k(k-1)p_k F_{\hat{\theta}}\left(\frac{1}{k}\right) > z \end{aligned} \tag{5.1.7}$$

which is precisely the global cascade condition proposed in [123]. This corresponds to a discontinuous transition with $\nu$ as order parameter and $\mu$ as control parameter at $\mu_c = 0$ (sublinear fraction size in the thermodynamic limit), as showcased in Figure 5.1a.

To characterise the discontinuous transition in general, we transform Eq.(5.1.5) into

$$\mu = \frac{\nu - h(\nu)}{1 - h(\nu)} \tag{5.1.8}$$

$\left.\frac{d\mu}{d\nu}\right|_0 < 0$ if and only if $h'(0) > 1$, as is the case pinpointed in Eq.(5.1.7). If there exists $0 < \nu_c < 1$ such that $\frac{d\mu}{d\nu} > 0$, $\forall \nu \in [0, \nu_c)$ and $\left.\frac{d\mu}{d\nu}\right|_{\nu_c} = 0$, then Eq.(5.1.8) describes a one-to-one mapping for $\nu \in [0, \nu_c)$. As such, $\nu$ continuously grows with $\mu$ until $\mu_c = \frac{\nu_c - h(\nu_c)}{1 - h(\nu_c)}$ where $\left.\frac{d\nu}{d\mu}\right|_c \to \infty$, indicating a discontinuous jump as shown in Figure 5.1b. The critical point $(\mu_c, \nu_c)$ satisfies

$$(1 - \mu_c)h'(\nu_c) = 1 \tag{5.1.9}$$

The extended global cascade conditions proposed in [124, 125] provide good approximations to the discontinuous transition when $\mu_c \approx 0$.

The jump vanishes when the critical point is an inflection point of the curve described by Eq.(5.1.8), as demonstrated in Figure 5.1c. The network parameters (e.g., mean degree $z$ and mean threshold $\theta$) fulfilling the requirement $\left.\frac{d^2\mu}{d\nu^2}\right|_c = 0$ thus give rise to the critical line or phase boundary

$$h''(\nu_c) = 0 \tag{5.1.10}$$

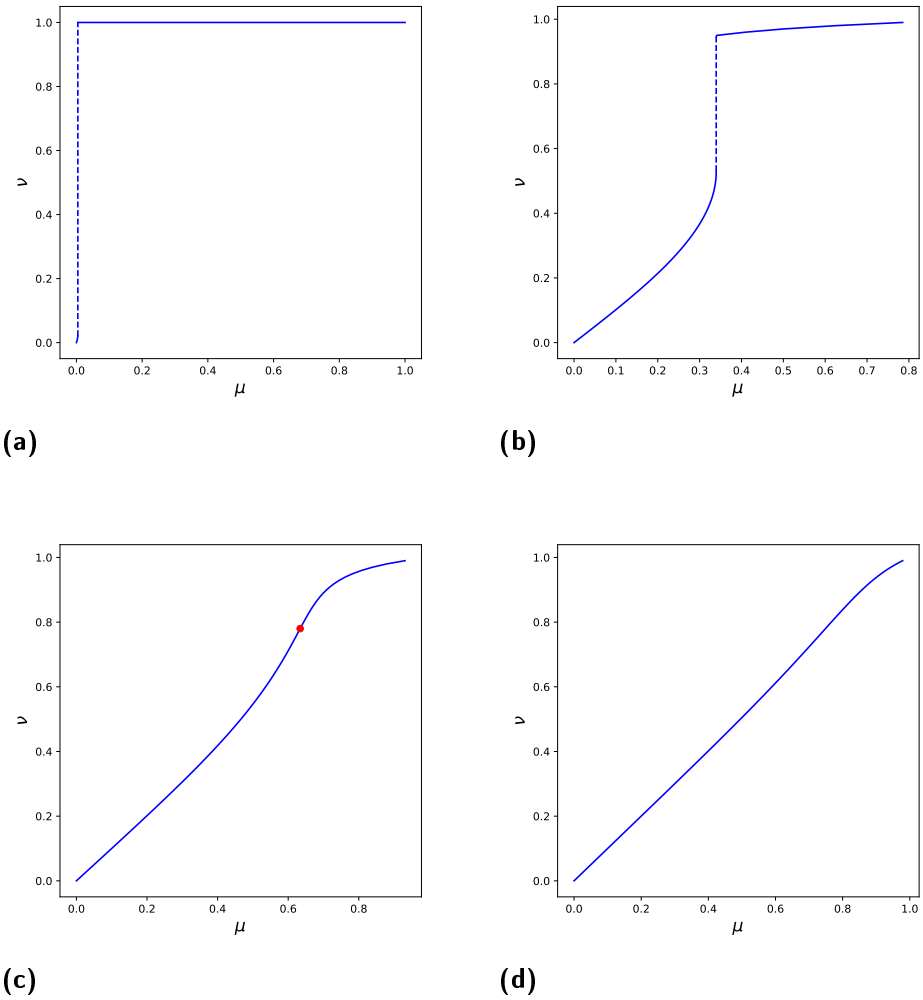



**Figure 5.1:** Examples of $\mu$ vs. $\nu$, ER networks with $z = 5$, fixed fractional threshold $\hat{\theta} \equiv \theta$

separating parameter regions with and without the discontinuous transition. When the threshold level is higher than that prescribed by the critical line, $\nu$ continuous grows with $\mu$ in $[0, 1)$, as exemplified in Figure 5.1d.

The analysis above focuses on the dependence of the average message $\nu$ on trigger size $\mu$. From Eq.(5.1.4) it is obvious that the final cascade size $\rho$ admits a discontinuous transition with respect to $\mu$ at $\mu_c$ if and only if $\nu$ does at $\mu_c$. Therefore, we propose Eq.(5.1.10) as *generalised cascade condition*,

together with the global cascade condition Eq.(5.1.7) depicting the phase diagram of WTM, as demonstrated in Figure 5.2. We consider WTM on Erdos–Renyi networks parameterised by mean degree $z$ and fixed fractional threshold $\hat{\theta} \equiv \theta$. Critical lines Eq.(5.1.7) (equality) and Eq.(5.1.10) are found numerically, marking out three phases which are termed *fragile*, *quasi-robust* and *robust* respectively, regarding the resilience of networks in each phase against threshold cascades of damage. Colours in the fragile and quasi-robust phases of Figure 5.2 are generated from Monte Carlo simulations of WTM on ER networks of size $N = 10^5$ with matching parameters over 100 realisations, brighter color for larger cascade size jump.

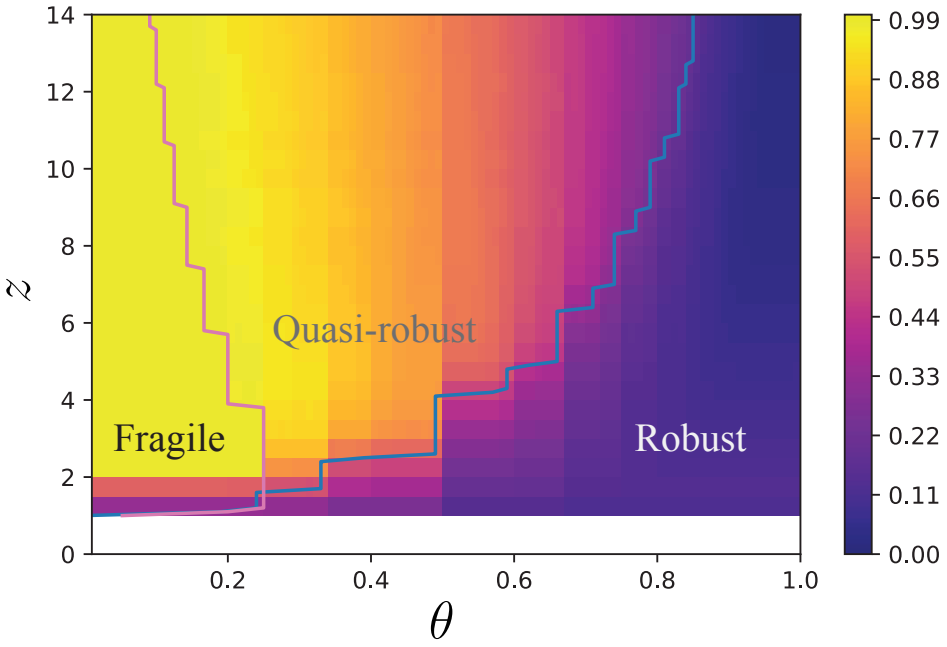



**Figure 5.2:** Phase diagram of WTM on ER networks

The discontinuous transition described above is in fact *hybrid*, i.e., exhibiting the critical behaviours of a second order phase transition before the jump $\mu \uparrow \mu_c$, similar in nature as bootstrap percolations [134] where the threshold for spreading is a fixed number of occupied neighbours. The critical exponent $\beta$ defined by $|\delta\rho| \sim |\delta\mu|^\beta$, $\mu \uparrow \mu_c$ can be obtained by taking variations on both sides of Eq.(5.1.4) and Eq.(5.1.5) and expanding to third order terms

and plugging in Eq.(5.1.9) and Eq.(5.1.10)

$$\delta\nu = \delta\mu + (1-\mu_c)\left[h'(\nu_c)\delta\nu + \frac{h''(\nu_c)}{2}(\delta\nu)^2 + \frac{h'''(\nu_c)}{6}(\delta\nu)^3\right] - \delta\mu\cdot h(\nu_c) \tag{5.1.11}$$

$$\delta\rho = \delta\mu\left[1-g(\nu_c)\right] + (1-\mu_c)\left[g'(\nu_c)\delta\nu + \frac{g''(\nu_c)}{2}(\delta\nu)^2 + \frac{g'''(\nu_c)}{6}(\delta\nu)^3\right] \tag{5.1.12}$$

The results, $\beta = 1/2$ in the quasi-robust phase and $\beta = 1/3$ on the phase boundary, are mean-field exponents. Since message-passing methods assume locally tree-like topology, on network ensembles in the thermodynamic limit, long-range dynamical correlations are effectively ignored.

### 5.1.2 WTM on fixed finite network

Now we shift our attention to WTM on a fixed finite network $G = (V, E)$ of size $N_1 = |V|$. Each link $(i, j) \in E$ corresponds to two directions for message-passing $i \leftarrow j$ and $j \leftarrow i$, totalling $N_2 = 2|E|$. Let $\mu$ be the probability of each node initially being damaged (equivalent trigger size). The threshold cascades of WTM can be approximated by the message-passing scheme similar to Eq.(5.1.1) and Eq.(5.1.2)

$$\boldsymbol{\rho}^{(t+1)} = \mu\mathbf{1}_{N_1} + (1-\mu)\boldsymbol{g}(\boldsymbol{\nu}^{(t)}) \tag{5.1.13}$$

$$\boldsymbol{\nu}^{(t+1)} = \mu\mathbf{1}_{N_2} + (1-\mu)\boldsymbol{h}(\boldsymbol{\nu}^{(t)}) \tag{5.1.14}$$

where $\boldsymbol{\rho}^{(t)}$ is a size $N_1$ vector with entries $\rho_j^{(t)}$ as the probability of node $j$ being damaged by time $t$, $\boldsymbol{\nu}^{(t)}$ a size $N_2$ vector with entries $\nu_{i\leftarrow j}^{(t)}$ as the expected message passed on from $j$ to $i$ at time $t$, and mappings $\boldsymbol{g} : [0,1]^{N_2} \mapsto [0,1]^{N_1}$

and $\boldsymbol{h} : [0,1]^{N_2} \mapsto [0,1]^{N_2}$ prescribed by

$$g_i(\boldsymbol{\nu}) = \sum_{m=1}^{\infty} \mathbb{P}\{\hat{m}_i < m\} \sum_{\substack{\Omega \subseteq \partial i \\ |\Omega|=m}} \prod_{j' \in \Omega} \nu_{i \leftarrow j'} \prod_{j'' \in \partial i \setminus \Omega} (1 - \nu_{i \leftarrow j''})$$
$$= \sum_{m=1}^{\infty} F_{\hat{\theta}}\left(\frac{m}{k_j}\right) \sum_{\substack{\Omega \subseteq \partial i \\ |\Omega|=m}} \prod_{j' \in \Omega} \nu_{i \leftarrow j'} \prod_{j'' \in \partial i \setminus \Omega} (1 - \nu_{i \leftarrow j''}) \tag{5.1.15}$$

$$h_{i \leftarrow j}(\boldsymbol{\nu}) = \sum_{m=1}^{\infty} F_{\hat{\theta}}\left(\frac{m}{k_j}\right) \sum_{\substack{\Omega \subseteq \partial j \setminus \{i\} \\ |\Omega|=m}} \prod_{l' \in \Omega} \nu_{j \leftarrow l'} \prod_{\substack{l'' \in \partial j \\ \setminus \Omega \cup \{i\}}} (1 - \nu_{j \leftarrow l''}) \tag{5.1.16}$$

Take $t$ to infinity and assume the iteration limit of Eq.(5.1.14) starting with $\boldsymbol{\nu}^{(0)} = \mu \mathbf{1}_{N_2}$ exists, we have

$$\boldsymbol{\rho} = \mu \mathbf{1}_{N_1} + (1 - \mu)\boldsymbol{g}(\boldsymbol{\nu}) \tag{5.1.17}$$
$$\boldsymbol{\nu} = \mu \mathbf{1}_{N_2} + (1 - \mu)\boldsymbol{h}(\boldsymbol{\nu}) \tag{5.1.18}$$

The final cascade probability vector $\boldsymbol{\rho} := \boldsymbol{\rho}^{(\infty)}$ qualitatively follows the expected message vector $\boldsymbol{\nu} := \boldsymbol{\nu}^{(\infty)}$ in relation to the trigger probability $\mu$ and sums up to the final cascade size $\rho := \sum_{i \in V} \rho_i$.

Eq.(5.1.18) is self-consistent but not easy to solve directly. To better understand the relationship between $\mu$ and $\boldsymbol{\nu}$, define $\boldsymbol{\Psi}(\boldsymbol{x}, \mu) := \mu \mathbf{1}_{N_2} + (1-\mu)\boldsymbol{h}(\boldsymbol{x})$, then Eq.(5.1.14) can be rewritten as

$$\boldsymbol{\nu}^{(t+1)} = \boldsymbol{\Psi}(\boldsymbol{\nu}^{(t)}, \mu) \tag{5.1.19}$$

The Jacobian matrix of $\boldsymbol{\Psi}(\mathbf{x}, \mu)$ which linearises Eq.(5.1.19) is given by

$$\mathbf{J}(\boldsymbol{\Psi}) = \left[\frac{\partial \boldsymbol{\Psi}}{\partial \boldsymbol{x}}\right] = (1 - \mu)\left[\frac{\partial \boldsymbol{h}}{\partial \boldsymbol{x}}\right], \tag{5.1.20}$$

where

$$\left[\frac{\partial \boldsymbol{h}}{\partial \boldsymbol{x}}\right]_{i\leftarrow j,j'\leftarrow l} = \delta_{jj'}(1-\delta_{il})\sum_{m=1}^{\infty}\left[F_{\hat{\theta}}\left(\frac{m}{k_j}\right) - F_{\hat{\theta}}\left(\frac{m-1}{k_j}\right)\right] \cdot \sum_{\substack{\Omega'\subseteq\partial j\setminus\{i\cup l\}\\ |\Omega'|=m-1}}\prod_{l'\in\Omega'} x_{j\leftarrow l'}\prod_{\substack{l''\in\partial j\\ \setminus\Omega'\cup\{i\cup l\}}}(1-x_{j\leftarrow l''}) \tag{5.1.21}$$

To characterise the evolution of expected messages $\boldsymbol{\nu}^{(t)}$ at the initial stage (of iterations), we evaluate the Jacobian at $\mu\mathbf{1}_{N_2}$, the message vector at arbitrary trigger size $\mu$.

$$J_{i\leftarrow j,j'\leftarrow l} = (1-\mu)B_{i\leftarrow j,j'\leftarrow l}\sum_{m=1}^{\infty}\triangle F_{\hat{\theta}}\left(\frac{m}{k_j}\right)\mathrm{Bin}(m-1,k_j-2;\mu) \tag{5.1.22}$$

where $\mathbf{B}$ is the non-backtracking matrix of graph $G$ with entries $B_{i\leftarrow j,j'\leftarrow l} = \delta_{jj'}(1-\delta_{il})$, $\triangle F_{\hat{\theta}}(\frac{m}{k_j}) = F_{\hat{\theta}}(\frac{m}{k_j}) - F_{\hat{\theta}}(\frac{m-1}{k_j})$ and $\mathrm{Bin}(m-1,k_j-2;\mu) = \binom{k_j-2}{m-1}\mu^{m-1}(1-\mu)^{k_j-m-1}$. Notice that the summation part in the right hand side of Eq.(5.1.22) has only index $j$ dependence, signifying the intermediate node that relays the message, we can define a $N_2\times N_2$ diagonal matrix $\mathbf{D}$ with entries $D_{i\leftarrow j,i\leftarrow j}$ the $j$ dependent sum aforementioned and rewrite Eq.(5.1.22) in a concise form:

$$\mathbf{J}|_{\mu\mathbf{1}_{N_2}} = (1-\mu)\mathbf{DB} \tag{5.1.23}$$

When $\mu = 0$, $D_{i\leftarrow j,i\leftarrow j} = F_{\hat{\theta}}(\frac{1}{k_j})$, Eq.(5.1.23) is reduced to the situation considered in Section 4.1 of [126].

The condition for explosive growth of message hence damage is given by the largest eigenvalue of the Jacobian matrix at $t = 0$ as expressed in Eq.(5.1.23). When $\lambda_M := \max\{\lambda[\mathbf{J}|_{\mu\mathbf{1}_{N_2}}]\}$ is larger than unity, the expected message grow exponentially in the initial iterations. Since the higher the threshold level the harder it is for cascades to spread, we suggest $\theta_c(\mu)$ satisfying $\lambda_M \uparrow 1$ as $\theta = \langle\hat{\theta}\rangle \downarrow \theta_c$ be the *critical threshold criterion* for the given triggering probability $\mu$. For a fixed finite network, the largest $\theta_c(\mu)$ for all $\mu \in [0,1)$ is analogous to the phase boundary of the quasi-robust phase in the network ensemble scenario.

We illustrate our results in Figure 5.3, for both synthetic and empirical networks. For simplicity we choose threshold condition $\hat{\theta} \equiv \theta$, hence $D_{i \leftarrow j, i \leftarrow j} = \mathrm{Bin}(m_j - 1, k_j - 2; \mu)$ and $m_j = [k_j \theta]$. Figure 5.3a and Figure 5.3c plot the $\mu \mapsto \theta_c$ relation described above from the eigenvalues of $\mathbf{J}|_{\mu \mathbf{1}_{N_2}}$ numerically found, for the Facebook Caltech network [135] and the configuration model based on the same degree sequence respectively; Figure 5.3b and Figure 5.3d show Monte Carlo simulation results of WTM on the same networks as used in their left panels. For chosen threshold level $\theta$, the abrupt transition is expected to happen around the triggering probability $\mu$ that makes $\theta$ critical, which can be found in the left panels Figure 5.3a and Figure 5.3c. The results are in good consistence with our prediction.

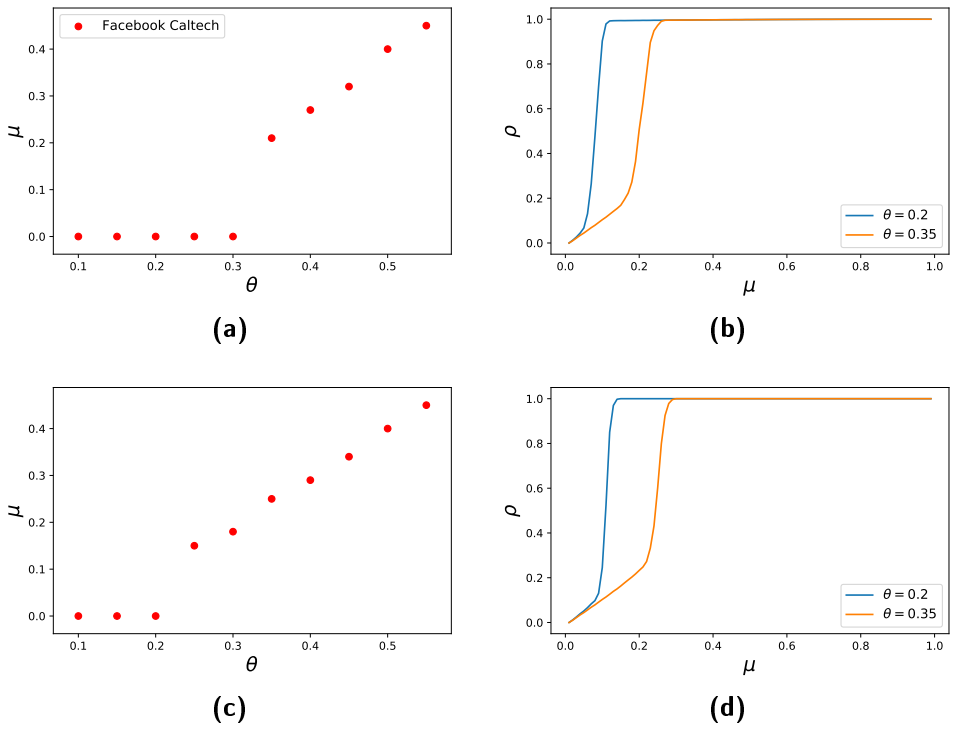



**Figure 5.3:** WTM on fixed finite network

## 5.2 Persistent Threshold Dynamics with Recovery on Random Networks

Some real-world networks, while being less susceptible to global cascade for small initial trigger, may be subject to persistently triggered cascades and some recovery mechanism. Typically, cascades happen in a much shorter time-scale than the intermittency of triggering or recovery. Such systems follow the dynamical patterns as: *triggering* $\rightarrow$ *cascading* $\rightarrow$ *triggering* (& *recovery*) $\rightarrow$ *cascading* $\rightarrow \cdots$, which are observed in a variety of social [136, 117, 137, 138], technical [121, 139, 140, 141], financial [142, 143, 120] and biological networks [144, 122]. The original WTM with one-off triggering can be viewed as the first step in the persistent picture: *triggering* $\rightarrow$ *cascading*. To characterise persistent threshold dynamics analytically is of great interest to network scientists, but it is also challenging due to the cumulative correlations built up in the dynamics. Some recent attempts have been made either by setting up models in a convenient way to harness the one-off results [143, 120, 145], or disregarding the separation of time-scales and considering continuous-time dynamics [146, 147, 148, 149].

In this section, we investigate a minimalistic model of persistent threshold dynamics with recovery based on WTM. Using results on WTM from **subsection 5.1.1** as building blocks and exploiting the structural features exposed during the persistent dynamics, we provide an approximation scheme which enables a good theoretical characterisation of the model. As our model is very generic and the theoretical approach can be easily extended to more complicated set-ups, this work contributes to the important quest of understanding networked systems which slowly evolve to the point of critical

collapse (or outburst in terms of spreading).

### 5.2.1 Model set-up and general behaviour

We consider the natural extension of WTM to persistent dynamics on random network ensemble with degree distribution $\{p_k\}$. Same as in WTM, each node can take a state of either damaged or undamaged and the initial configuration starts with all nodes undamaged; Each node is assigned with a fractional threshold, for simplicity assume to be fixed at $\theta$.

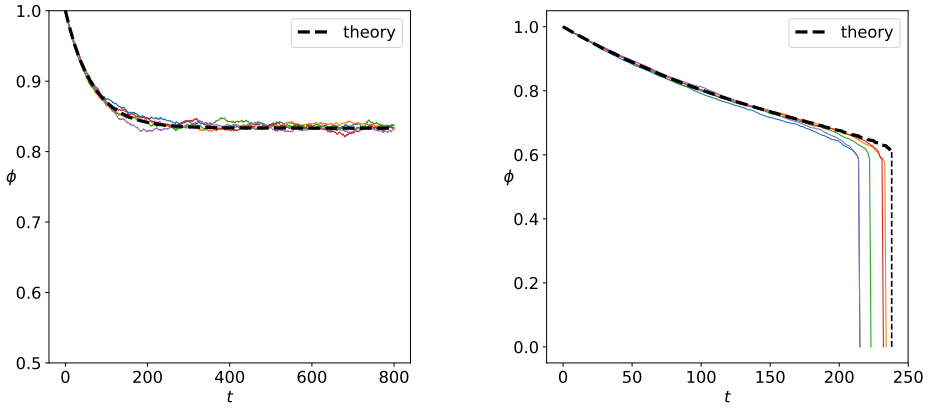
The persistent dynamics occur at two separate time-scales: spontaneous damage (triggering) and recovery at the slow or macroscopic time-scale, and cascading via the dynamical rules of WTM at the fast or microscopic time-scale. More precisely, take discrete time-steps at the macroscopic scale and denote them by $t$, the dynamics goes as follows:

(i) In each time-step, undamaged / damaged nodes are subject to spontaneous damage / recovery independently with small probability $r_0$ or $r_1$ respectively. Define the ratio $R := r_1/r_0$, which can be interpreted as the relative intensity of recovery over triggering.

(ii) In addition, undamaged nodes (after the updates in (i)) are subject to cascading as in WTM, i.e, an undamaged node turns damaged if among its neighbours the damaged ones exceed the fractional threshold. The (average) fraction of damaged nodes after cascading stops in time-step $t$ is the damage fraction at $t$, denoted as $\rho(t)$ while the undamaged fraction as $\phi(t) := 1 - \rho(t)$. The dynamics then continues to time-step $t + 1$.

Further, we limit our attention to the persistent dynamics on quasi-robust random networks, a general class of networks proposed in **subsection 5.1.1**, since on robust networks cascading is less relevant and on fragile networks one-off small trigger suffices to damage almost the entire network. In general, the temporal evolution of undamaged fraction $\phi(t)$ (from the context

of network resilience) exhibits one of the two types of behaviour depending on chosen $R$: decreasing to an intermediate value and fluctuating around it for large $R$, or gradually dropping before suddenly collapsing to a much lower value for small $R$. We refer to them as the *stationary phase* and the *collapsing phase* respectively, as showcased in Figure 5.4.




**(a)** Stationary phase, high recovery **(b)** Collapsing phase, low recovery

**Figure 5.4:** Illustration of two phases of networks under the persistent dynamics

The temporal evolution of undamaged fraction of nodes $\phi(t)$ for persistent dynamics with recovery on Poisson random networks with mean degree $z = 30$, fixed fractional threshold $\theta = 0.5$, triggering rate $r_0 = 0.0025$ and recovery rate $r_1 = R{\cdot}r_0$; (a) $R = 5$ (b) $R = 1$. Starting from fully undamaged initial configuration $\phi = 1$, five realisations are shown as thin colourful lines in both (a)&(b), while thick black dash lines are theoretical calculations follow from the analysis below.

### 5.2.2 Effective trigger size evolution of the persistent dynamics

In order to theoretically characterise the persistent dynamics on quasi-robust networks, it would be tempting to replace the increasing trigger size $\mu$ in the analysis in **subsection 5.1.1** with the temporal evolution of some effective trigger size $\mu_e(t)$. Here we argue that by classifying the damaged nodes

in the persistent dynamics into two types: spontaneously damaged nodes and nodes damaged via cascading, under certain assumptions the spontaneously damaged nodes can indeed serve as effective trigger $\mu_e(t)$ to estimate the network damage fraction $\rho(t)$.

Assume that when the network (either in stationary or collapsing phase) evolves in low damage regime, spontaneously damaged nodes that fall below the sustainable condition are negligible. This means that all spontaneously damaged nodes are recoverable. Further we assume that all nodes damaged via cascading accumulated over time are mostly below the sustainable condition. Since we have small probabilities per time-step $r_0, r_1 \ll 1$, the second assumption would thus infer that nodes damaged via cascading are much less likely to be recovered (or may only recover at much slower pace) compared to spontaneously damaged nodes. The above assumptions are reasonable in all cases considered in this work, and are believed to hold for quasi-robust networks in general.

The theoretical estimation of the persistent process is given by the following *effective process*: In each time-step, (i) Each undamaged node is spontaneously damaged with probability $r_0$ and each spontaneously damaged node recovers with probability $r_1$, both independently; (ii) The updated spontaneously damaged nodes serve as the *effective trigger* and govern the cascading according to the threshold dynamical rule of WTM. In other words, it is the alternating combination of "independent spontaneous damage / recovery of undamaged / spontaneous damaged node" and "refreshing of cascading damage". It is worth pointing out that the different treatment of two types of damaged nodes here is not because of enforced intrinsic properties of damage, as is the case in [143]), but is a result due to their different positioning in the network hence their susceptibility to recovery. Figure 5.5 provides a schematic illustration of the effective dynamics.

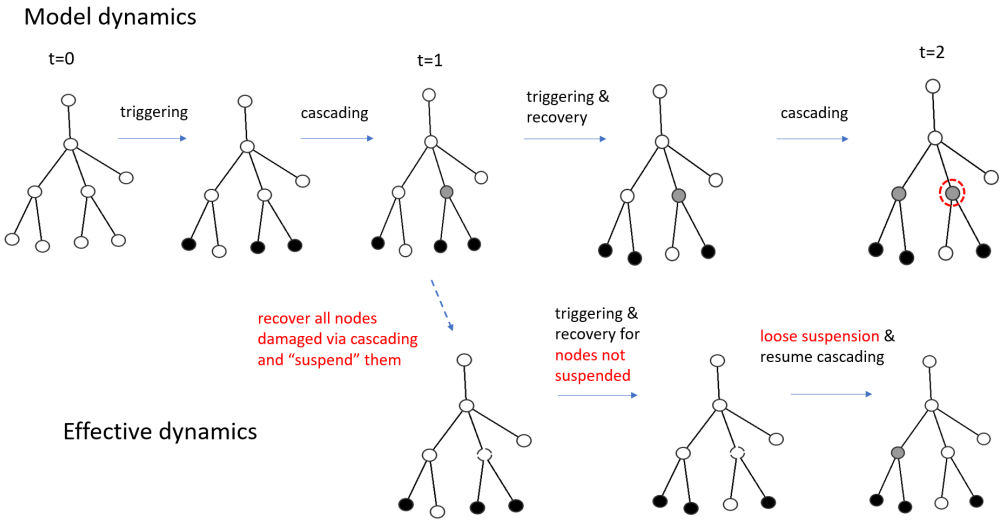



**Figure 5.5:** Schematic illustration of the effective dynamics in contrast to the model dynamics

Example of a possible realisation of the model dynamics (upper panel) and the corresponding effective dynamics (lower panel). Empty nodes with solid boundary are active nodes, black for spon-failed nodes, grey for cas-failed nodes. Empty nodes with dashed boundary are cas-failed nodes put in cavity, i.e., perceived as active nodes during the updates between two macroscopic time-steps.

Using results from the trigger size analysis for expected cascading damage, the rate equation of the effective trigger size $\mu_e(t)$ is given by

$$\begin{aligned} \frac{\mathrm{d}\mu_e}{\mathrm{d}t} &= r_0[1-\hat{\rho}(\mu_e)] - r_1\mu_e \\ \mu_e(0) &= 0, \end{aligned} \tag{5.2.1}$$

where $\hat{\rho}(\bullet)$ stands for the mapping from the trigger size $\mu$ to the final cascade size $\rho$ in WTM, as encoded in Eq.(5.1.4) and Eq.(5.1.5) The estimation of undamaged fraction at time $t$ (before the critical collapse for networks in the collapsing phase or without constraint in the stationary phase) is thus

$$\rho(t) = \hat{\rho}(\mu_e(t)), \tag{5.2.2}$$

where $\mu_e(t)$ evolves according to Eq.(5.2.1).

If taking $\mathrm{d}\mu_e/\mathrm{d}t = 0$ in Eq.(5.2.1) gives a physical stationary state, we say the network belongs to the stationary phase. At the stationary state, denote $\mu_e^* := \mu_e(\infty)$ and $\rho^* := \hat{\rho}(\mu_e^*)$. Eq.(5.2.1) indicates that the stationary damage fraction $\rho^*$ only depends on the ratio $R = r_1/r_0$ as defined earlier. For high $R$ which ensures stationary phase, this dependence relation can be illustrated from Figure 5.6, at the intersection of left hand side $\hat{\rho}(\mu_e)$ (blue line) and right hand side $1 - R\mu_e$ (red dashed line).

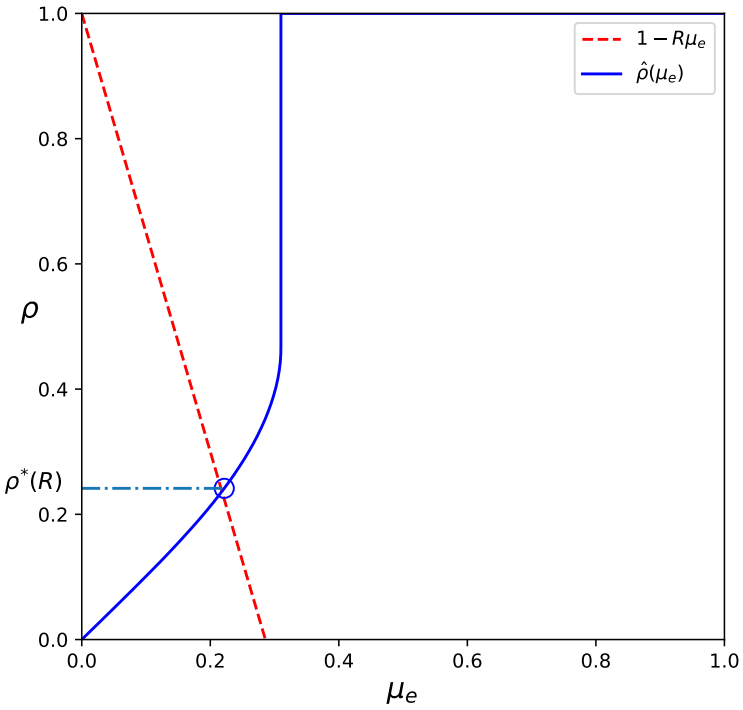



**Figure 5.6:** $\rho(R)$ from effective trigger size of steady state

Dynamics on Poisson random networks with degree distribution $p_k = e^{-z}z^k/k!$, $z = 10$ and fractional threshold $\theta = 0.5$, the estimation of steady state death fraction $\rho$ given relative recovery intensity $R$, shown here for $R = 3.5$.

Figure 5.6 also shows that $\mu_e^*$ monotonically increases as $R$ decreases. Given that the mapping $r\hat{h}o : mu \mapsto \rho$ holds up to $\mu = \mu_c$ with the critical trigger size of WTM $\mu_c$ prescribed by Eq.(5.1.9), we can define

$$R_c := [1 - \hat{\rho}(\mu_c)]/\mu_c \tag{5.2.3}$$

as the critical (recovery over damage) ratio. The network is expected to be in the stationary phase when $R > R_c$ and in the collapsing phase when $R < R_c$. For networks in the collapsing phase, the effective trigger size would evolve in the form of Eq.(5.2.1), increasing until reaching $\mu_c$. Thus we can identify the time of collapse $t_c$ as the solution of the boundary value problem: Eq.(5.2.1) with additional end-time condition

$$\mu_e(t_c) = \mu_c. \tag{5.2.4}$$

### 5.2.3 Results and discussions

Calculations based on the effective process introduced above are conducted to compare with Monte Carlo simulation results. Estimates for the temporal evolution of undamaged fraction are plotted in thick black dash lines in Figure 5.4, in good agreement with simulation results for both the stationary phase and pre-collapse stage of the collapsing phase.

Take a decreasing set of large $R$ values and record the average stationary damage fraction in the state for each $R$. Results are shown by the red dots in Figure 5.7, with detailed parameters in figure comments. Blue lines represent the theoretical estimates $\rho^*(R)$ of the same set of $R$ values. Theory and simulations agree with convincing accuracy for networks safely in the active phase ($R \gg R_c$), regardless of network structure. As $R$ approaches the theoretical critical point $R_c$ from above, deviations for the stationary damage fraction kick in. One can see that the more homogeneous random networks are and the more mean degrees they have (Poisson random network with mean degree $z = 30$), the better the estimates extend to the regime closer to the critical

collapse. Nevertheless, in all cases the actual critical point found in simulations is larger than its theoretical estimate $R_c$. In other words, theoretical estimate $R_c$ provides a lower bound, below which the network would safely belong to the collapsing phase. This can be explained by further scrutiny over the effective dynamics in comparison with the model dynamics, see Figure 5.6. As the theoretical damage fraction $\rho(t)$ (for any given $R$) is derived from the effective trigger size $\mu_e(t)$, the *recoverable* cascading damaged nodes, i.e., nodes damaged via cascading earlier, but at the current time-step satisfy the sustainable condition due to accumulated neighbour recovery, are considered to be recovered with *certainty* in the effective dynamics, but not necessarily so in the model dynamics. For lower $R$, the damage fraction would increase such that this fraction of nodes becomes no longer negligible. Therefore, it is to be expected that the theoretical damage fraction is an *underestimation*, and in simulations networks are prone to collapse for some $R > R_c$.

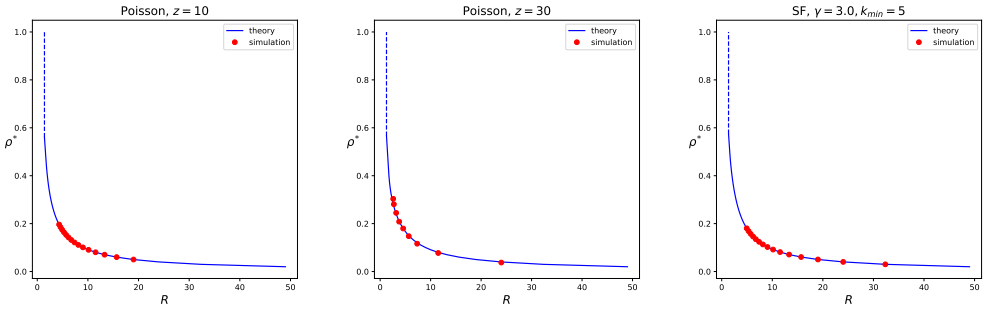



**Figure 5.7:** $R$ vs. $\rho^*$ in the stationary phase, theoretical estimates and simulation results
(a) & (b) Poisson random networks with $z = 10$ and $z = 30$ respectively;
(c) Scale-free random networks with $p_k \propto k^{-\gamma}$, $\gamma = 3.0$, $k_{\min} = 5$, $\langle k \rangle \approx 8.7$. In all cases we fix $\theta = 0.5$ and $r_0 = 0.0025$.

For networks in the collapsing phase ($R < R_c$), we can also calculate the time of collapse $t_c$, and compare with results from simulations, as shown in Figure 5.8. Blue lines plotted from theoretical estimate, while red dots with error bars are average and standard deviation of $t_c$ from simulations. In all cases theory and simulations are in reasonable alignment, with $t_c$ being an

expected upper bound. Following the same argument in the last paragraph, since the estimated damage fraction being underestimation, the actual time of collapse comes earlier than the theoretically predicted one.

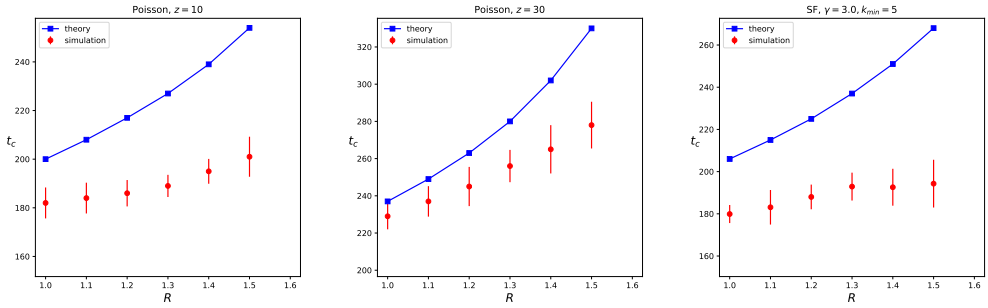



**Figure 5.8:** $R$ vs. $t_c$ in the collapsing phase, theoretical estimates and simulation results

(a) & (b) Poisson random networks with $z = 10$ and $z = 30$ respectively; (c) Scale-free random networks with $p_k \propto k^{-\gamma}$, $\gamma = 3.0$, $k_{\min} = 5$, $\langle k \rangle \approx 8.7$. In all cases we fix $\theta = 0.5$ and $r_0 = 0.0025$.

In this section we develop a method to calculate the average damage fraction of complex networks under cascade-recovery dynamics if the recovery is strong enough to keep the network "functional" (largely undamaged), and the collapsing time for the damage to spread to the bulk of the network if otherwise. The simulation results are in good consistency with our theoretical estimates, with moderate discrepancies closer to critical point of collapse, as a result of optimistic approximation of recoverable nodes damaged via threshold cascading from past time. Therefore, the critical ratio $R_c$ predicted by our method can be used as a necessary lower bound for recovery to avoid critical collapse and the predicted collapsing time $t_c$ a upper bound of the longevity of the system.

From the perspective of application, our model can be potentially applied to predict the collapsing time of complex systems with interdependency, or the condition for it to remain functional. For example, the stock market in

which the performance of the stock of each company depends on its upstream-downstream partners, while the 0 and 1 states of each company correspond to debt deficit status and debt solvent status respectively [142, 143, 120]. Our method then can be used to predict whether the collapse of the entire stock market could be triggered by the chain reaction of debt deficits of listed companies based on enterprise financing efficiency and disbursement rate. Similarly, with our method we could also try to predict the lifespan of some animal [122], the collapsing time and condition of honey bee colonies [150], the failure time of power grids [151], the behaviour of progression of lung carcinomas with different cell proliferation and apoptosis rates [144], the spread of disruptions in railway systems [140], the collective behaviour in online social movements [137], and so forth. In general, our model has a strong potential in characterising a variety of complex systems with binary state components and network structure, on which non-monotone dynamics are running, and we are going to explore those candidate systems in future study.

# 6

# Summary

In this thesis we examine and explore a number of theoretical methods for stochastic particle systems, especially reaction particle systems. Our general approach is to study effective mean-field theories that are exactly solvable probabilistic models which retain as much information of the original dynamics as possible, as well as to utilise field-theoretic methods to go beyond mean-field theories.

In **Chapter 1** and **Chapter 2**, we discuss different classes of non-spatial and spatial branching processes as candidates for non-trivial mean-field theories, some of which are largely ignored in the physics literatures and go against popular presumptions for mean-field theories of non-equilibrium systems [12, 24]. Some new results on the temporal profile of branching particle systems are obtained, which may serve as refined characterisation of critical avalanches.

In **Chapter 3**, we showcase incorporating short-range dynamical correlations of the Abelian Manna Model in an effective multi-type branching

process that is exactly solvable, yielding closed-form approximates of the critical density of the Abelian Manna Model in generic set-ups, which previously are only available from numerical simulations, semi-numerical analysis, or in the brute mean-field value.

In **Chapter 4**, we introduce and develop field-theoretic methods to tackle long-range dynamical correlations of reaction particle systems, with application in branching Wiener Sausage and extension to particle systems on graphs. The last part of Chapter 4 for field-theoretic methods on graphs is still in preliminary form and worth further investigation.

Finally in **Chapter 5**, we adapt the message-passing method on networks for variants of the classical Watts Threshold Model, and explain how message-passing is fundamentally an effective mean-field theory tailored to ignore dynamical correlations on networks.

# Bibliography


[1] Mehran Kardar. *Statistical physics of particles*. Cambridge University Press, 2007.

[2] Pavel L Krapivsky, Sidney Redner, and Eli Ben-Naim. *A kinetic view of statistical physics*. Cambridge University Press, 2010.

[3] Yaneer Bar-Yam. General features of complex systems. *Encyclopedia of Life Support Systems (EOLSS), UNESCO, EOLSS Publishers, Oxford, UK*, 1, 2002.

[4] James Ladyman, James Lambert, and Karoline Wiesner. What is a complex system? *European Journal for Philosophy of Science*, 3(1):33–67, 2013.

[5] Crispin Gardiner. *Stochastic methods*. Springer Berlin, 2009.

[6] Fred Brauer, Carlos Castillo-Chavez, and Carlos Castillo-Chavez. *Mathematical models in population biology and epidemiology*, volume 2. Springer, 2012.

[7] Paul Adrien Maurice Dirac. *The principles of quantum mechanics*. Number 27. Oxford university press, 1981.

[8] Thomas Liggett. *Interacting particle systems*, volume 276. Springer Science & Business Media, 2012.

[9] Thomas M Liggett. *Stochastic interacting systems: contact, voter and exclusion processes*, volume 324. Springer Science & Business Media, 2013.

[10] Anthony CC Coolen, Reimer Kühn, and Peter Sollich. *Theory of neural information processing systems*. OUP Oxford, 2005.

[11] Romualdo Pastor-Satorras, Claudio Castellano, Piet Van Mieghem, and Alessandro Vespignani. Epidemic processes in complex networks. *Reviews of modern physics*, 87(3):925, 2015.

[12] Malte Henkel, Haye Hinrichsen, Sven Lübeck, and Michel Pleimling. *Non-equilibrium phase transitions*, volume 1. Springer, 2008.

[13] Haye Hinrichsen. Non-equilibrium critical phenomena and phase transitions into absorbing states. *Advances in physics*, 49(7):815–958, 2000.

[14] Sven Lübeck. Universal scaling behavior of non-equilibrium phase transitions. *International Journal of Modern Physics B*, 18(31n32):3977–4118, 2004.

[15] Uwe C Täuber. *Critical dynamics: a field theory approach to equilibrium and non-equilibrium scaling behavior*. Cambridge University Press, 2014.

[16] Martin A Nowak. *Evolutionary dynamics: exploring the equations of life*. Harvard university press, 2006.

[17] Alain Barrat, Marc Barthelemy, and Alessandro Vespignani. *Dynamical processes on complex networks*. Cambridge university press, 2008.

[18] Mason Porter and James Gleeson. *Dynamical systems on networks: A tutorial*, volume 4. Springer, 2016.

[19] Heinz Georg Schuster. *Criticality in neural systems*. John Wiley & Sons, 2014.

[20] Henrik Jeldtoft Jensen. *Self-organized criticality: emergent complex behavior in physical and biological systems*, volume 10. Cambridge university press, 1998.

[21] Gunnar Pruessner. *Self-organised criticality: theory, models and characterisation*. Cambridge University Press, 2012.

[22] Nicholas W Watkins, Gunnar Pruessner, Sandra C Chapman, Norma B Crosby, and Henrik J Jensen. 25 years of self-organized criticality: Concepts and controversies. *Space Science Reviews*, 198(1-4):3–44, 2016.

[23] Krishna B Athreya and Peter E Ney. *Branching processes*, volume 196. Springer Science & Business Media, 2012.

[24] Miguel A Munoz. Colloquium: Criticality and dynamical scaling in living systems. *Reviews of Modern Physics*, 90(3):031001, 2018.

[25] Nanxin Wei and Gunnar Pruessner. Comment on "finite-size scaling of survival probability in branching processes". *Physical Review E*, 94(6):066101, 2016.

[26] James P Sethna, Karin A Dahmen, and Christopher R Myers. Crackling noise. *Nature*, 410(6825):242, 2001.

[27] James P Gleeson and Rick Durrett. Temporal profiles of avalanches on networks. *Nature Communications*, 8(1):1227, 2017.

[28] Jonathan Touboul and Alain Destexhe. Power-law statistics and universal scaling in the absence of criticality. *Physical Review E*, 95(1):012413, 2017.

[29] Ali Faqeeh, Saeed Osat, Filippo Radicchi, and James P Gleeson. Emergence of power laws in noncritical neuronal systems. *Physical Review E*, 100(1):010401, 2019.

[30] Ronald Dickman, Alessandro Vespignani, and Stefano Zapperi. Self-organized criticality as an absorbing-state phase transition. *Physical Review E*, 57(5):5095, 1998.

[31] Ronald Dickman, Miguel A Muñoz, Alessandro Vespignani, and Stefano Zapperi. Paths to self-organized criticality. *Brazilian Journal of Physics*, 30(1):27–41, 2000.

[32] Theodore E Harris. *The theory of branching processes*. Courier Corporation, 2002.

[33] Patsy Haccou, Patricia Haccou, Peter Jagers, Vladimir A Vatutin, and Vladimir Vatutin. *Branching processes: variation, growth, and extinction of populations*. Number 5. Cambridge university press, 2005.

[34] David Axelrod and Marek Kimmel. *Branching processes in biology.* Springer-Verlag, 2015.

[35] Richard Durrett. Branching process models of cancer. In *Branching process models of cancer*, pages 1–63. Springer, 2015.

[36] Richard Courant and David Hilbert. *Methods of Mathematical Physics: Partial Differential Equations.* John Wiley & Sons, 2008.

[37] Philippe Flajolet and Andrew Odlyzko. Singularity analysis of generating functions. *SIAM Journal on discrete mathematics*, 3(2):216–240, 1990.

[38] Boris Alexandrovich Sevast'yanov. Age-dependent branching processes. *Theory of Probability & Its Applications*, 9(4):521–537, 1964.

[39] Boris Alexandrovich Sevast'yanov. Limit theorems for age-dependent branching processes. *Theory of Probability & Its Applications*, 13(2):237–259, 1968.

[40] Martin I Goldstein. Critical age-dependent branching processes: single and multitype. *Zeitschrift für Wahrscheinlichkeitstheorie und Verwandte Gebiete*, 17(1):74–88, 1971.

[41] Peter Jagers et al. *Branching processes with biological applications.* Wiley, 1975.

[42] Serena di Santo, Pablo Villegas, Raffaella Burioni, and Miguel A Munoz. Simple unified view of branching process statistics: Random walks in balanced logarithmic potentials. *Physical Review E*, 95(3):032115, 2017.

[43] Juan A Bonachela, Sebastiano De Franciscis, Joaquín J Torres, and Miguel A Munoz. Self-organization without conservation: are neuronal avalanches generically critical? *Journal of Statistical Mechanics: Theory and Experiment*, 2010(02):P02015, 2010.

[44] John M Beggs and Nicholas Timme. Being critical of criticality in the brain. *Frontiers in physiology*, 3:163, 2012.

[45] Matteo Martinello, Jorge Hidalgo, Amos Maritan, Serena Di Santo, Dietmar Plenz, and Miguel A Munoz. Neutral theory and scale-free neural dynamics. *Physical Review X*, 7(4):041071, 2017.

[46] Martin Meyer, Shlomo Havlin, and Armin Bunde. Clustering of independently diffusing individuals by birth and death processes. *Physical Review E*, 54(5):5567, 1996.

[47] William R Young, Anthony J Roberts, and Gordan Stuhne. Reproductive pair correlations and the clustering of organisms. *Nature*, 412(6844):328, 2001.

[48] Bahram Houchmandzadeh. Clustering of diffusing organisms. *Physical Review E*, 66(5):052902, 2002.

[49] Andrea Zoia, Eric Dumonteil, Alain Mazzolo, Clélia de Mulatier, and Alberto Rosso. Clustering of branching Brownian motions in confined geometries. *Physical Review E*, 90(4):042118, 2014.

[50] Louis-Pierre Arguin, Anton Bovier, and Nicola Kistler. The extremal process of branching Brownian motion. *Probability Theory and related fields*, 157(3-4):535–574, 2013.

[51] Zhan Shi. *Branching Random Walks: École d'Été de Probabilités de Saint-Flour XLII–2012*, volume 2151. Springer, 2016.

[52] Anton Bovier. *Gaussian processes on trees: From spin glasses to branching Brownian motion*, volume 163. Cambridge University Press, 2017.

[53] Mark Kot, Jan Medlock, Timothy Reluga, and D Brian Walton. Stochasticity, invasions, and branching random walks. *Theoretical population biology*, 66(3):175–184, 2004.

[54] Stanley Sawyer. Branching diffusion processes in population genetics. *Advances in Applied Probability*, 8(4):659–689, 1976.

[55] Eric Dumonteil, Satya N Majumdar, Alberto Rosso, and Andrea Zoia. Spatial extent of an outbreak in animal epidemics. *Proceedings of the National Academy of Sciences*, 110(11):4239–4244, 2013.

[56] Ellen Powell. An invariance principle for branching diffusions in bounded domains. *Probability Theory and Related Fields*, 173(3-4):999–1062, 2019.

[57] Simon Harris and Matthew Roberts. The many-to-few lemma and multiple spines. In *Annales de l'Institut Henri Poincaré, Probabilités et Statistiques*. University of Bath, 2015.

[58] Simon C Harris, Marion Hesse, Andreas E Kyprianou, et al. Branching Brownian motion in a strip: survival near criticality. *The Annals of Probability*, 44(1):235–275, 2016.

[59] Walter Wyss. The fractional diffusion equation. *Journal of Mathematical Physics*, 27(11):2782–2785, 1986.

[60] Harry Kesten. Branching Brownian motion with absorption. *Stochastic Processes and their Applications*, 7(1):9–47, 1978.

[61] Julien Berestycki, Nathanaël Berestycki, and Jason Schweinsberg. Survival of near-critical branching Brownian motion. *Journal of Statistical Physics*, 143(5):833–854, 2011.

[62] Julien Berestycki, Nathanaël Berestycki, Jason Schweinsberg, et al. The genealogy of branching Brownian motion with absorption. *The Annals of Probability*, 41(2):527–618, 2013.

[63] Julien Berestycki, Nathanaël Berestycki, and Jason Schweinsberg. Critical branching Brownian motion with absorption: survival probability. *Probability Theory and Related Fields*, 160(3-4):489–520, 2014.

[64] Julien Berestycki, Nathanael Berestycki, Jason Schweinsberg, et al. Critical branching Brownian motion with absorption: particle configurations. In *Annales de l'Institut Henri Poincaré, Probabilités et Statistiques*, volume 51, pages 1215–1250. Institut Henri Poincaré, 2015.

[65] Nanxin Wei and Gunnar Pruessner. Critical density of the Abelian Manna model via a multitype branching process. *Physical Review E*, 100(3):032116, 2019.

[66] SS Manna. Two-state model of self-organized criticality. *Journal of Physics A: Mathematical and General*, 24(7):L363, 1991.

[67] Per Bak, Chao Tang, and Kurt Wiesenfeld. Self-organized criticality. *Physical review A*, 38(1):364, 1988.

[68] Deepak Dhar. The abelian sandpile and related models. *Physica A: Statistical Mechanics and its Applications*, 263(1-4):4–25, 1999.

[69] Asa Ben-Hur and Ofer Biham. Universality in sandpile models. *Physical Review E*, 53(2):R1317, 1996.

[70] Deepak Dhar. Some results and a conjecture for Manna's stochastic sandpile model. *Physica A: Statistical Mechanics and its Applications*, 270(1-2):69–81, 1999.

[71] Ronald Dickman. n-site approximations and coherent-anomaly-method analysis for a stochastic sandpile. *Physical Review E*, 66(3):036122, 2002.

[72] Urna Basu and PK Mohanty. Self-organised criticality in stochastic sandpiles: Connection to directed percolation. *EPL (Europhysics Letters)*, 108(6):60002, 2014.

[73] Kay Jörg Wiese. Coherent-state path integral versus coarse-grained effective stochastic equation of motion: From reaction diffusion to stochastic sandpiles. *Physical Review E*, 93(4):042117, 2016.

[74] Gary Willis and Gunnar Pruessner. Spatio-temporal correlations in the Manna model in one, three and five dimensions. *International Journal of Modern Physics B*, 32(05):1830002, 2018.

[75] Kim Christensen, Álvaro Corral, Vidar Frette, Jens Feder, and Torstein Jøssang. Tracer dispersion in a self-organized critical system. 77(1):107–110, 1996.

[76] Maya Paczuski and Stefan Boettcher. Universality in sandpiles, interface depinning, and earthquake models. 77(1):111–114, 1996.

[77] Michela Rossi, Romualdo Pastor-Satorras, and Alessandro Vespignani. Universality class of absorbing phase transitions with a conserved field. *Physical review letters*, 85(9):1803, 2000.

[78] Henrik Jeldtoft Jensen. Lattice gas as a model of 1/f noise. 64(26):3103–3106, Jun 1990.

[79] S Lübeck. Moment analysis of the probability distribution of different sandpile models. *Physical Review E*, 61(1):204, 2000.

[80] Ronald Dickman, Mikko Alava, Miguel A Munoz, Jarkko Peltola, Alessandro Vespignani, and Stefano Zapperi. Critical behavior of a one-dimensional fixed-energy stochastic sandpile. *Physical Review E*, 64(5):056104, 2001.

[81] Hoai Nguyen Huynh, Gunnar Pruessner, and Lock Yue Chew. The Abelian Manna model on various lattices in one and two dimensions. *Journal of Statistical Mechanics: Theory and Experiment*, 2011(09):P09024, 2011.

[82] Hoai Nguyen Huynh and Gunnar Pruessner. Abelian Manna model in three dimensions and below. *Physical Review E*, 85(6):061133, 2012.

[83] Preben Alstrøm. Mean-field exponents for self-organized critical phenomena. *Physical Review A*, 38(9):4905, 1988.

[84] Ricardo García-Pelayo. Dimension of branching processes and self-organized criticality. *Physical Review E*, 49(6):4903, 1994.

[85] Stefano Zapperi, Kent Bækgaard Lauritsen, and H Eugene Stanley. Self-organized branching processes: mean-field theory for avalanches. *Physical review letters*, 75(22):4071, 1995.

[86] Dranreb Earl Juanico, Christopher Monterola, and Caesar Saloma. Dissipative self-organized branching in a dynamic population. *Physical Review E*, 75(4):045105, 2007.

[87] Juan A Bonachela and Miguel A Munoz. Self-organization without conservation: true or just apparent scale-invariance? *Journal of Statistical Mechanics: Theory and Experiment*, 2009(09):P09009, 2009.

[88] Maya Paczuski and Kevin E. Bassler. Theoretical results for sandpile models of SOC with multiple topplings. 2000.

[89] Gunnar Pruessner. The average avalanche size in the Manna model and other models of self-organized criticality. *International Journal of Modern Physics B*, 27(05):1350009, 2013.

[90] Gunnar Pruessner and Ole Peters. Self-organized criticality and absorbing states: Lessons from the Ising model. 73(2):025106(R)–1–4, 2006.

[91] Anne Fey, Lionel Levine, and David B. Wilson. Driving sandpiles to criticality and beyond. 104(14):145703, Apr 2010.

[92] Béla Bollobás and Bollobás Béla. *Random graphs*. Number 73. Cambridge university press, 2001.

[93] Alessandro Vespignani, Ronald Dickman, Miguel A Munoz, and Stefano Zapperi. Absorbing-state phase transitions in fixed-energy sandpiles. *Physical Review E*, 62(4):4564, 2000.

[94] Mahashweta Basu, Urna Basu, Sourish Bondyopadhyay, P. K. Mohanty, and Haye Hinrichsen. Fixed-energy sandpiles belong generically to directed percolation. 109:015702, Jul 2012.

[95] Daniel Hexner and Dov Levine. Hyperuniformity of critical absorbing states. *Physical review letters*, 114(11):110602, 2015.

[96] Ronald Dickman, Tânia Tomé, and Mário J De Oliveira. Sandpiles with height restrictions. *Physical Review E*, 66(1):016111, 2002.

[97] Torgny Lindvall. *Lectures on the coupling method*. Courier Corporation, 2002.

[98] Ignacio Bordeu, Saoirse Amarteifio, Rosalba Garcia-Millan, Benjamin Walter, Nanxin Wei, and Gunnar Pruessner. Volume explored by a branching random walk on general graphs. *Scientific reports*, 9(1):1–9, 2019.

[99] Daniel J Amit and Victor MartíN-Mayor. *Field Theory, the Renormalization Group, and Critical Phenomena: Graphs to Computers*. World Scientific Press, 2005.

[100] Masao Doi. Stochastic theory of diffusion-controlled reaction. *Journal of Physics A: Mathematical and General*, 9(9):1479, 1976.

[101] L Peliti. Path integral approach to birth-death processes on a lattice. *J. Physique*, 46:1469–1483, 1985.

[102] Nicolaas Godfried Van Kampen. *Stochastic processes in physics and chemistry*, volume 1. Elsevier, 1992.

[103] Uwe C Täuber, Martin Howard, and Benjamin P Vollmayr-Lee. Applications of field-theoretic renormalization group methods to reaction–diffusion problems. *Journal of Physics A: Mathematical and General*, 38(17):R79, 2005.

[104] John Cardy. Reaction-diffusion processes. lectures at Warwick University, 2006.

[105] Michael E Peskin. *An introduction to quantum field theory*. CRC press, 2018.

[106] Naoki Masuda, Mason A Porter, and Renaud Lambiotte. Random walks and diffusion on networks. *Physics reports*, 716:1–58, 2017.

[107] Fan RK Chung and Fan Chung Graham. *Spectral graph theory*. Number 92. American Mathematical Soc., 1997.

[108] Bojan Mohar and Wolfgang Woess. A survey on spectra of infinite graphs. *Bulletin of the London Mathematical Society*, 21(3):209–234, 1989.

[109] AN Samukhin, SN Dorogovtsev, and JFF Mendes. Laplacian spectra of, and random walks on, complex networks: Are scale-free architectures really important? *Physical Review E*, 77(3):036115, 2008.

[110] Patrick N McGraw and Michael Menzinger. Laplacian spectra as a diagnostic tool for network structure and dynamics. *Physical Review E*, 77(3):031102, 2008.

[111] Sune Lehmann and Yong-Yeol Ahn. *Complex spreading phenomena in social systems*. Springer, 2018.

[112] Damon Centola, Víctor M Eguíluz, and Michael W Macy. Cascade dynamics of complex propagation. *Physica A: Statistical Mechanics and its Applications*, 374(1):449–456, 2007.

[113] Damon Centola and Michael Macy. Complex contagions and the weakness of long ties1. *American journal of Sociology*, 113(3):702–734, 2007.

[114] Li Chen, Fakhteh Ghanbarnejad, Weiran Cai, and Peter Grassberger. Outbreaks of coinfections: The critical role of cooperativity. *EPL (Europhysics Letters)*, 104(5):50001, 2013.

[115] Weiran Cai, Li Chen, Fakhteh Ghanbarnejad, and Peter Grassberger. Avalanche outbreaks emerging in cooperative contagions. *Nature physics*, 11(11):936, 2015.

[116] Damon Centola. The spread of behavior in an online social network experiment. *science*, 329(5996):1194–1197, 2010.

[117] Márton Karsai, Gerardo Iniguez, Kimmo Kaski, and János Kertész. Complex contagion process in spreading of online innovation. *Journal of The Royal Society Interface*, 11(101):20140694, 2014.

[118] Zhongyuan Ruan, Gerardo Iniguez, Márton Karsai, and János Kertész. Kinetics of social contagion. *Physical review letters*, 115(21):218702, 2015.

[119] Thomas R Hurd and James P Gleeson. On watts' cascade model with random link weights. *Journal of Complex Networks*, 1(1):25–43, 2013.

[120] Boris Podobnik, D Horvatic, Mário Augusto Bertella, L Feng, X Huang, and B Li. Systemic risk in dynamical networks with stochastic failure criterion. *EPL (Europhysics Letters)*, 106(6):68003, 2014.

[121] Markus Schläpfer and Jonathan L Shapiro. Modeling failure propagation in large-scale engineering networks. *Complex Sciences*, pages 2127–2138, 2009.

[122] Dervis C Vural, Greg Morrison, and L Mahadevan. Aging in complex interdependency networks. *Physical Review E*, 89(2):022811, 2014.

[123] Duncan J Watts. A simple model of global cascades on random networks. *Proceedings of the National Academy of Sciences*, 99(9):5766–5771, 2002.

[124] James P Gleeson and Diarmuid J Cahalane. An analytical approach to cascades on random networks. In *SPIE Fourth International Symposium on Fluctuations and Noise*, pages 66010W–66010W. International Society for Optics and Photonics, 2007.

[125] James P Gleeson and Diarmuid J Cahalane. Seed size strongly affects cascades on random networks. *Physical Review E*, 75(5):056103, 2007.

[126] James P Gleeson and Mason A Porter. Message-passing methods for complex contagions. *arXiv preprint arXiv:1703.08046*, 2017.

[127] James P Gleeson. Cascades on correlated and modular random networks. *Physical Review E*, 77(4):046117, 2008.

[128] Adam Hackett, Sergey Melnik, and James P Gleeson. Cascades on a class of clustered random networks. *Physical Review E*, 83(5):056107, 2011.

[129] Adam Hackett and James P Gleeson. Cascades on clique-based graphs. *Physical Review E*, 87(6):062801, 2013.

[130] Osman Yaugan and Virgil Gligor. Analysis of complex contagions in random multiplex networks. *Physical Review E*, 86(3):036103, 2012.

[131] Charles D Brummitt, Kyu-Min Lee, and K-I Goh. Multiplexity-facilitated cascades in networks. *Physical Review E*, 85(4):045102, 2012.

[132] Sen Pei, Xian Teng, Jeffrey Shaman, Flaviano Morone, and Hernán A Makse. Efficient collective influence maximization in cascading processes with first-order transitions. *Scientific reports*, 7:45240, 2017.

[133] Bailey K Fosdick, Daniel B Larremore, Joel Nishimura, and Johan Ugander. Configuring random graph models with fixed degree sequences. *SIAM Review*, 60(2):315–355, 2018.

[134] Gareth J Baxter, Sergey N Dorogovtsev, Alexander V Goltsev, and José FF Mendes. Bootstrap percolation on complex networks. *Physical Review E*, 82(1):011103, 2010.

[135] Amanda L Traud, Eric D Kelsic, Peter J Mucha, and Mason A Porter. Comparing community structure to characteristics in online collegiate social networks. *SIAM review*, 53(3):526–543, 2011.

[136] P Singh, S Sreenivasan, BK Szymanski, and G Korniss. Threshold-limited spreading in social networks with multiple initiators. *Scientific Reports*, 3:2330, 2013.

[137] Lada Adamic et al. The diffusion of support in an online social movement: Evidence from the adoption of equal-sign profile pictures. In *Proceedings of the 18th ACM Conference on Computer Supported Cooperative Work & Social Computing*, pages 1741–1750. ACM, 2015.

[138] Raquel Alvarez, David Garcia, Yamir Moreno, and Frank Schweitzer. Sentiment cascades in the 15m movement. *EPJ Data Science*, 4(1):6, 2015.

[139] Sergey V Buldyrev, Roni Parshani, Gerald Paul, H Eugene Stanley, and Shlomo Havlin. Catastrophic cascade of failures in interdependent networks. *Nature*, 464(7291):1025–1028, 2010.

[140] Jonas Johansson, Henrik Hassel, and Alexander Cedergren. Vulnerability analysis of interdependent critical infrastructures: case study of

the swedish railway system. *International journal of critical infrastructures*, 7(4):289–316, 2011.

[141] Walter Quattrociocchi, Guido Caldarelli, and Antonio Scala. Self-healing networks: redundancy and structure. *PloS one*, 9(2):e87986, 2014.

[142] Antonio Majdandzic, Boris Podobnik, Sergey V Buldyrev, Dror Y Kenett, Shlomo Havlin, and H Eugene Stanley. Spontaneous recovery in dynamical networks. *Nature Physics*, 10(1):34–38, 2014.

[143] B Podobnik, A Majdandzic, C Curme, Z Qiao, W-X Zhou, HE Stanley, and B Li. Network risk and forecasting power in phase-flipping dynamical networks. *Physical Review E*, 89(4):042807, 2014.

[144] JÜRGEN MATTERN and MANFRED VOLM. Imbalance of cell proliferation and apoptosis during progression of lung carcinomas. *Anticancer research*, 24(6):4243–4246, 2004.

[145] Boris Podobnik, Tomislav Lipic, Davor Horvatic, Antonio Majdandzic, Steven R Bishop, and H Eugene Stanley. Predicting the lifetime of dynamic networks experiencing persistent random attacks. *Scientific reports*, 5, 2015.

[146] LD Valdez, MA Di Muro, and LA Braunstein. Failure-recovery model with competition between failures in complex networks: a dynamical approach. *Journal of Statistical Mechanics: Theory and Experiment*, 2016(9):093402, 2016.

[147] Lucas Böttcher, Mirko Lukovic, Jan Nagler, Shlomo Havlin, and Hans J Herrmann. Impact of embedding on predictability of failure-recovery dynamics in networks. *arXiv preprint arXiv:1610.00997*, 2016.

[148] L Böttcher, M Luković, J Nagler, S Havlin, and HJ Herrmann. Failure and recovery in dynamical networks. *Scientific Reports*, 7:41729, 2017.

[149] Lucas Böttcher, Jan Nagler, and Hans J Herrmann. Critical behaviors in contagion dynamics. *Physical Review Letters*, 118(8):088301, 2017.

[150] Clint J Perry, Eirik Søvik, Mary R Myerscough, and Andrew B Barron. Rapid behavioral maturation accelerates failure of stressed honey bee colonies. *Proceedings of the National Academy of Sciences*, 112(11):3427–3432, 2015.

[151] Jian-Wei Wang and Li-Li Rong. Cascade-based attack vulnerability on the us power grid. *Safety Science*, 47(10):1332–1336, 2009.